University of Alberta

Studies on the improvement in wear resistance of WC-Co composites by adding a pseudo-elastic TiNi phase and relevant issues

by

Yang PAN

A thesis submitted to the Faculty of Graduate Studies and Research
in partial fulfillment of the requirements for the degree of

Master of Science
in
Materials Engineering

Department of Chemical and Materials Engineering

Spring 2012
Edmonton, Alberta

Abstract:

In this study, pseudo-elastic TiNi alloy was added as a second phase to the Co matrix of WC-Co composite, which has found many applications in forms of coating, hardfacing overlay and bulk against wear. It was demonstrated that the added TiNi phase markedly enhanced the wear resistance of WC-60%wtCo composite. However, the beneficial effect of the TiNi phase was diminished when the amount of added TiNi exceeded 10wt% due to the formation of pores.

The TiNi alloy was also directly used as the matrix to fabricate WC-TiNi and TiC-TiNi composites. The TiNi-matrix composites exhibited higher wear resistance than WC-Co composite when the volume fraction of the metal matrix was high, e.g., 60vol%. However, the situation was reversed when the volume fraction of the metal matrix was lowered. It appears that the formation of pores was also responsible for the deterioration of the TiNi-matrix composites.

Keywords: TiNi alloy, WC-Co composite, WC-TiNi, TiC-TiNi, wear, pseudo-elasticity

Acknowledgement

I am grateful for the conscientious instructions from my supervisor Dr. Dongyang Li during my master's program; besides, I appreciate the financial support from Natural Science and Engineering Research Council of Canada (NSERC) and Imperial Oil Canada Ltd..

Table of Contents

List of Tables

List of Figures

Chapter 1

Introduction

Chapter 1 - Introduction

In Chapter 1, a general introduction to the subject of wear is provided in the first section, followed by the introduction to properties of tungsten carbide cobalt (WC-Co) composite, titanium carbide (TiC), and titanium nickel (TiNi) alloy in the second section; in the third section, the main purpose of this study is addressed, and the content of other chapters is briefed at last.

1.1 Definition of wear

In early studies of this subject, wear was defined as the removal of materials from solid surfaces as a result of mechanical action [1]. However, as the research was deepened and the cases involving oxidation or corrosive wear arouse, it drawn the awareness that this definition shall not be limited within mechanical interaction. Thus, wear became better defined as the progressive loss of material from the operating surface(s) of one or more bodies occurring as a result of relative motion at the surface(s) [2], which may eventually result in failure of the materials in service.

1.1.1 The use of wear

From the definition, one can tell that wear is not desirable in engineering application in general, but there are also considerable usages of wear if this double-edged sword is handled properly. Take diamond rings as an example,

coarse diamonds cannot be admirable without proper cutting and polishing, and the polishing process involves abrasive wear; or the master-pieces of sketches for instance, sketches would not be realistic if graphite could not be “worn” on drawing papers. However, the engineering wear applications are far more complex and difficult to control when compared to these simple examples; therefore, the subject of wear should be investigated into more details.

1.1.2 Types of wear

Knowing that wear process might involve additional chemical reactions, it is divided into two main streams. One is summarized as the “mechanical wear”, the other one is wear in a reactive environment such as those with active chemical elements [3]. The former stream, i.e. the mechanical wear mode, can be generally sub-divided into four types, which are adhesive wear, abrasive wear, surface fatigue and erosion. Figure 1-1 depicts these four groups and the mechanism under each group in an ascending sequence of severity.

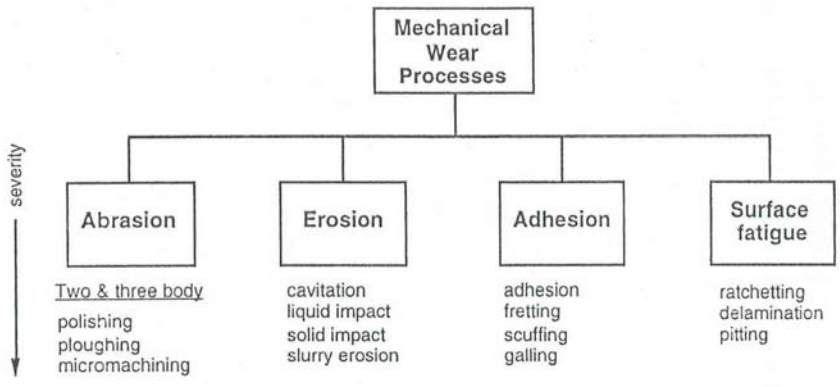

Fig. 1-1. A classification of mechanical wear processes [Ref. 3]

The second stream, wear in a reactive environment or corrosive wear, involves mechanical wear mechanism, chemical and/or electrochemical reactions along with influences of other external factors such as temperature, lubricant, or other contaminants [2].

Other than the above classification according to the mechanism, the wear situations can also be categorized for the purpose of selecting wear-resistant materials [2]. These are:

1. Sliding wear

2. Fretting

3. Three-body abrasion

4. Gouging wear

5. Low-stress abrasion

6. Erosion

7. Corrosive wear

In order to introduce difference types of wear from a theoretical point of view, the first classification is adopted for further elaboration.

1.1.2.1 Adhesive wear

Perfect flat surface is never achieved by preparation such as machining, grinding, polishing and etc, so all surfaces have asperities [4]. When two solid surfaces are placed against each other under load, only a very small region of the asperities will actually be in contact, while a large percentage of the nominal contact area is relatively further away from the corresponding surface, as shown in Fig 1-2. In the figure, it is obvious that the real contact area (A_r) is much smaller than the apparent contact area (A_a). As a result, the stress around those asperities areas (usually referred to as "junctions") could be considerably higher than the nominal stress, then the asperities will deform elastically and plastically if yielding occurs, also the local temperature could be significantly elevated.

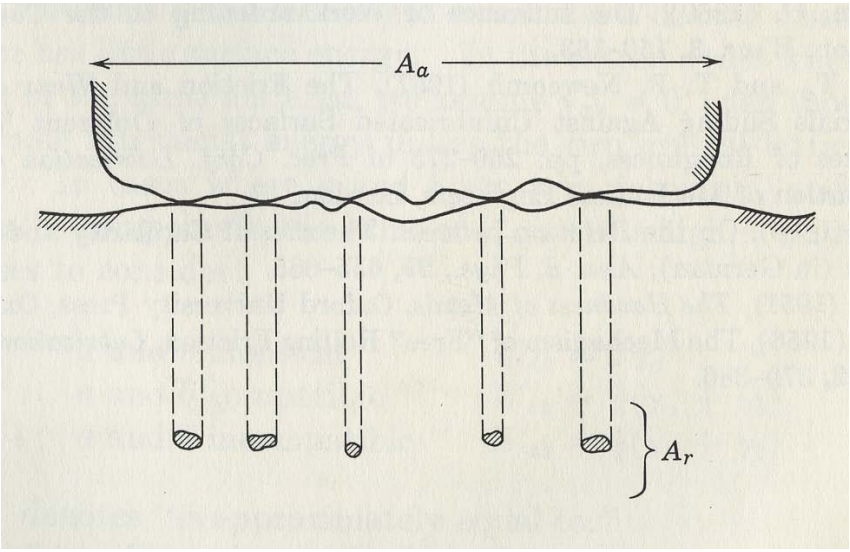

Fig. 1-2. Comparison of A_r to A_a in a schematic depiction of surfaces in contact [Ref. 1]

From a microscopic view, atoms on the asperities of the two surfaces are so close to each other that the atom-to-atom force takes place, and this attractive force leads to adhesion of the two surfaces. When atoms are transferred from its original surface to the other in contact, adhesive wear has occurred. Fig 1-3 and Fig 1-4 schematically illustrate the adhesion process [2]. If the adhesion strength of the junction is lower compared to the cohesive strength of either material in the contact pair, the junction will simply rupture in the original path, i.e. path 1 in Fig 1-4; if not, the junction will rupture in a new path within the material with lower cohesive strength, i.e. path 2 in the figure.

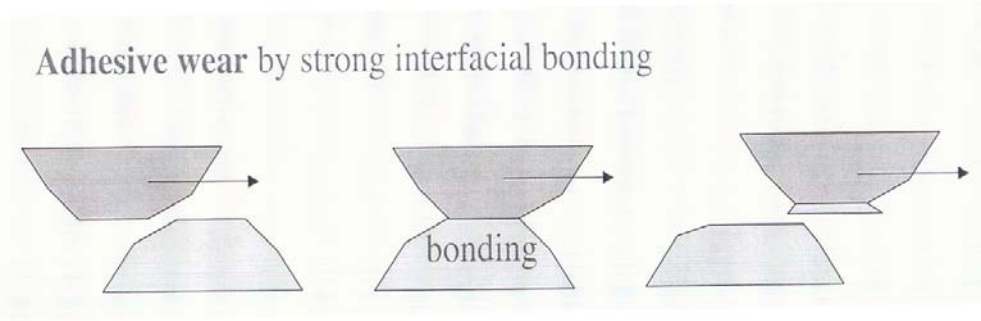

Fig. 1-3. Adhesive wear

The equation of volume loss of adhesive wear can be approximately expressed as

$$V=KWL/H \tag{1-1}$$

where V is the volume loss of adhesive wear, K is a wear coefficient, W is the normal load, L is the total distance of relative motion and H is the indentation hardness of the material being worn. This equation can be deduced as follows.

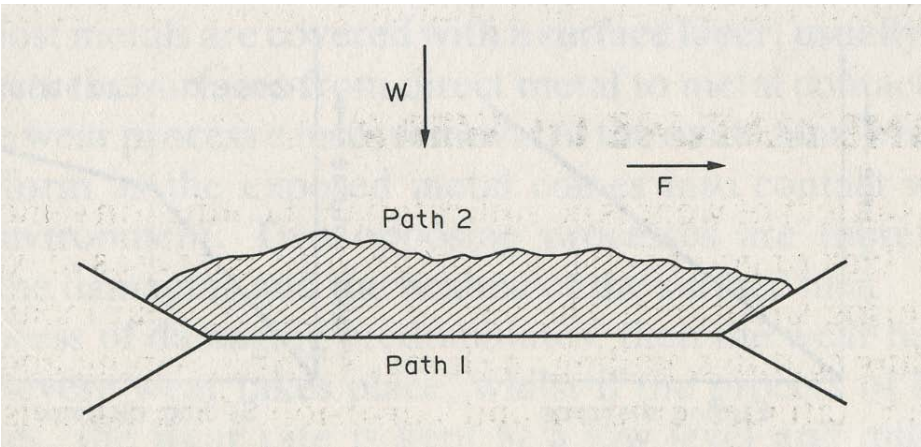

Fig. 1-4. Alternative rupture path after adhesion of surfaces [Ref. 2]

If the tips of the asperities are taken as spherical, the real area in contact will be proportional to the normal load, and the coefficient H is defined as load divided by the surface area in real contact (Fig 1-5) [5].

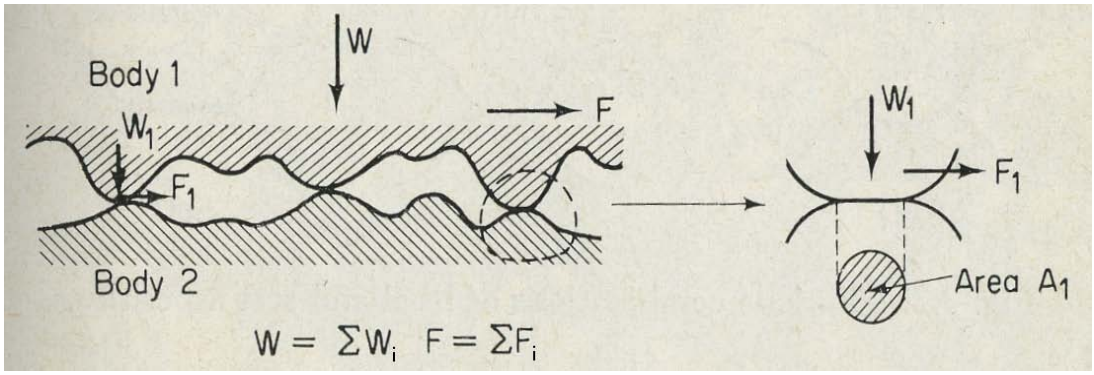

Fig. 1-5. Approximate assembly of local asperity contact [Ref.5]

$$A_1=W_1/H \qquad (1\text{-}2)$$

Since $W=\sum W_i$, and $A=\sum A_i$, it is obvious that

$$A_r = W/H \quad (1\text{-}3)$$

It is predictable that the adhesive wear loss is proportional to the real areas where adhesion occurred and the total distance of relative motion of the materials in contact, so $V \propto A_r \times L \propto W \times L/H$, where L is the distance of relative motion. Thus, the volume wear loss can be written in the form of equation 1-1.

There are several factors influencing adhesive wear [2]. Firstly, adhesive wear is mitigated when there is lubrication present or low shear-strength surface films on the hard materials. A second approach to weaken adhesive wear is to reduce the mutual solubility of the materials in contact. If the materials are mutually insoluble to each other, atom-to-atom force is less likely to take place at the asperities regions. Besides, fine grain size and possible HCP packing are desirable for lowering adhesive wear. Temperature has strong influence on adhesive wear. At elevated temperatures, the atomic interaction is enhanced and the contact area becomes larger due to softening of the material in contact, both increasing adhesive wear.

1.1.2.2 Abrasive wear

Abrasive wear occurs when two rough surfaces interact with each other, mainly involving mechanical interactions. During this process, plowing and cutting usually occur on the softer surface caused by hard asperities, and the removed

material becomes loose fragments [1]. This process is referred to as two-body abrasive wear as Fig.1-6 illustrates.

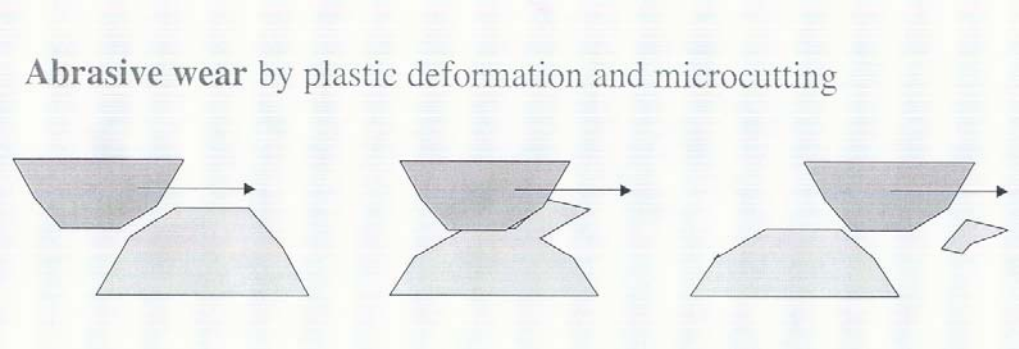

Fig. 1-6 Two-body abrasive wear

When there are hard loose particles between the mating pair of materials as grits, the removal of materials due to these hard particles is referred to as three-body abrasive wear [4]. Fig 1-7 shows the categories and situations of different mechanisms of abrasive wear.

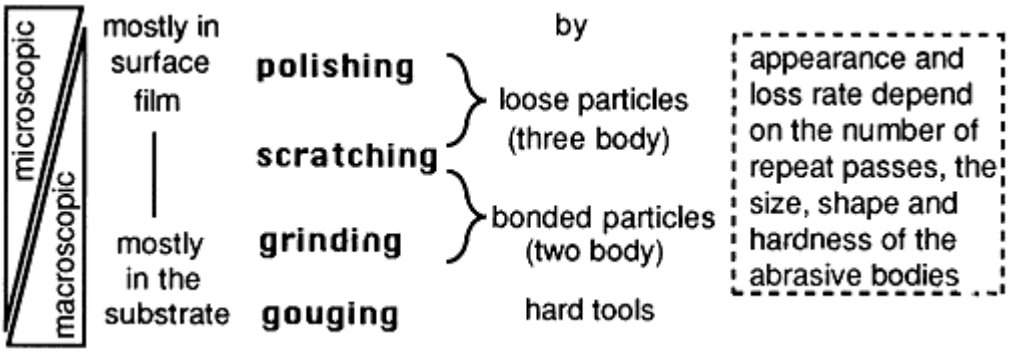

Fig. 1-7. Categories abrasive wear on size scale [Ref. 6]

In the case of two-body abrasive wear, the volume loss of abrasive wear can be expressed as

$$V=K_aWL/H \quad (1\text{-}4)$$

where V is the volume loss of adhesive wear, K_a is a wear coefficient, W is the normal load, L is the total distance of relative motion, and H is the hardness of the material being worn. Despite the similarity to the adhesive wear loss equation 1-1, it should be brought forward that the abrasive wear coefficient K_a has a much higher value than the adhesive wear coefficient K mentioned above [5].

In this two-body abrasive wear mode, surface roughness and hardness of material is of importance to the wear loss. It is obvious that hardness plays a role since the volume loss is inversely proportional to the hardness of the material. Better surface finishing, especially on the harder material, will reduce wear loss since it reduces the hard asperities and thus the possibility of cutting or plowing.

For three-body abrasive wear, measures can also be taken to reduce the wear loss. In industrial cases, it is difficult to control the geometry or hardness of abrading grits for they usually enter the system from the environment, so measures such as suitable sealing or filtration are taken to prevent external particles [5]. However, wear debris generated within the system is inevitable and it can accelerate the wear process. It is a greater problem than the external hard particles since the debris forms as the wear process continues, and cannot be excluded completely.

1.1.2.3 Surface fatigue

When subjected to cyclic loading and unloading, there will be a maximum shear stress forming below the surface [7], as shown in Fig 1-8; this shear stress can lead to nucleation of cracks and the propagation to the surface which causes the material to detach from the surface [4]. Fig 1-9 illustrates the early stage of surface fatigue wear, the initiation of the cracks are always from below the surface as shown.

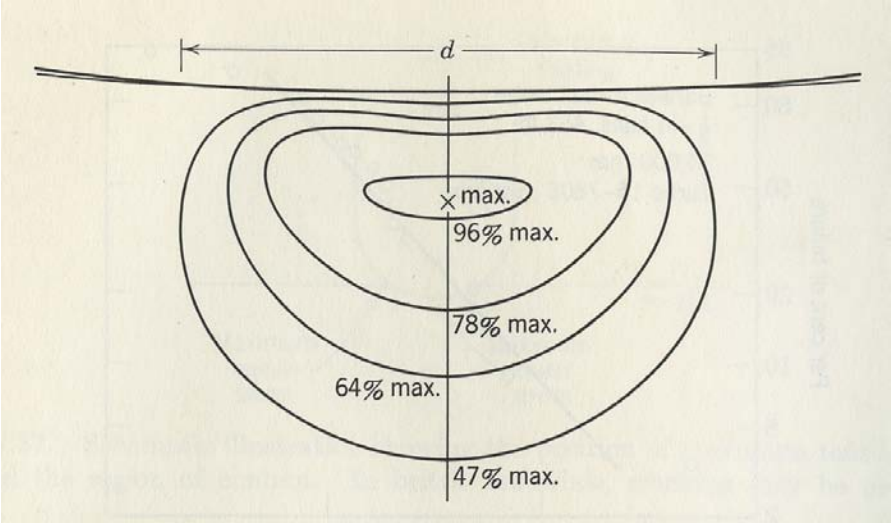

Fig. 1-8. Distribution of shear stress of surface if subjected to cyclic loading and unloading [Ref. 1].

It is worth noting that there is a remarkable difference between surface fatigue wear and the two wear modes mentioned above. Either of adhesive wear or abrasive wear requires loading condition and actual physical contact of two surfaces. While for surface fatigue wear, only cyclic loading and unloading is

demanded while physical contact may not be necessary. For instance, when there is proper lubricant present between the two surfaces under cyclic loading and unloading, adhesive wear or abrasive wear will be alleviated, but surface fatigue wear is still very likely to happen [5].

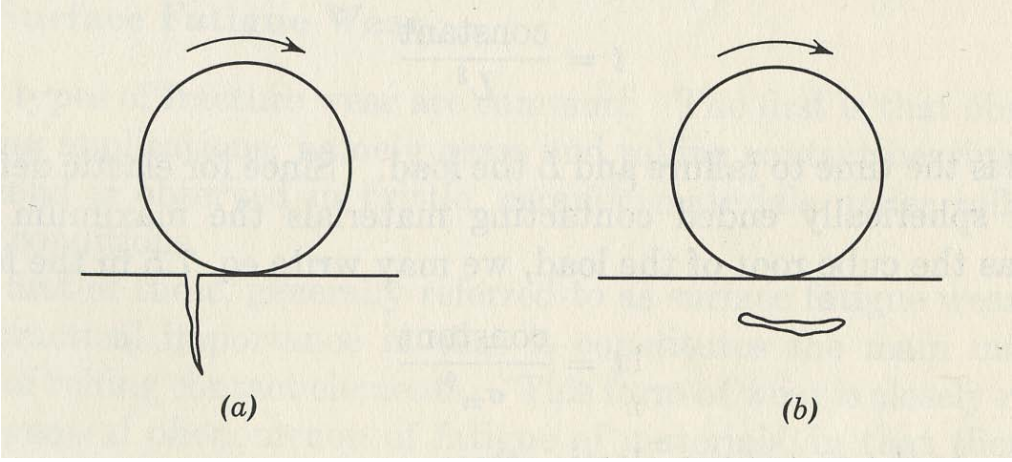

Fig. 1-9. Illustration of early stage in surface fatigue (a) Surface crack (b) Subsurface [Ref. 1]

1.1.2.4 Erosive wear

Erosive wear describes the damage resulted from the impingement of particles on surface of the object [2] as schematically illustrated in Fig.1-10. However, erosive wear may also happen due to flow of hot gases or cavitations of liquid media with

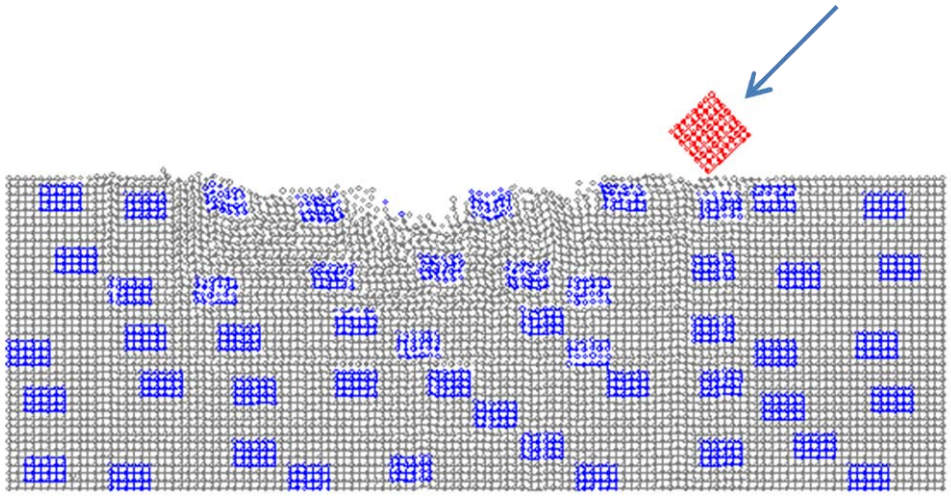

Fig. 1-10 Erosive wear caused by solid-particle impingement

collapsing bubbles. Sand blasting is an example of the application of erosive wear where the sharp particles are transported by compressed air, besides, erosive wear also occurs when the sharp particles are transported by flowing liquids, in which water jet cutting may be a proper example. In the case of hard particle impingement, the erosive wear is influenced by the following factors [8]: ductility of material being eroded, microstructure, velocity of particles, impingement angle, particle size, hardness of particles, strength of particles and temperature. For instance, small angle attacks are the most destructive for ductile material, while attacks with large angle (close to 90 degrees) wear the most on brittle materials [9].

1.1.2.5 Corrosive wear

Corrosive wear is referred to the wear in a reactive environment during which corrosion is involved and reaction products are worn off the surface [9].

In corrosive wear, there is corrosive attack of the surface first due to the reaction between the naked surface and the environment. If there is protective film formed, the wear rate could slow down after the first corrosion stage, as the protective film is worn away for the time being, new naked surface will be exposed and the process keeps repeating itself, thus the surface materials continuously become worn or corroded. On the other hand, if no protective film is formed or the film is so poor that it is worn away instantly after formation, the wear rate will be a summative effect of abrasive wear together with chemical corrosion. Fig. 1-11 demonstrates the wear rates of the two different scenarios.

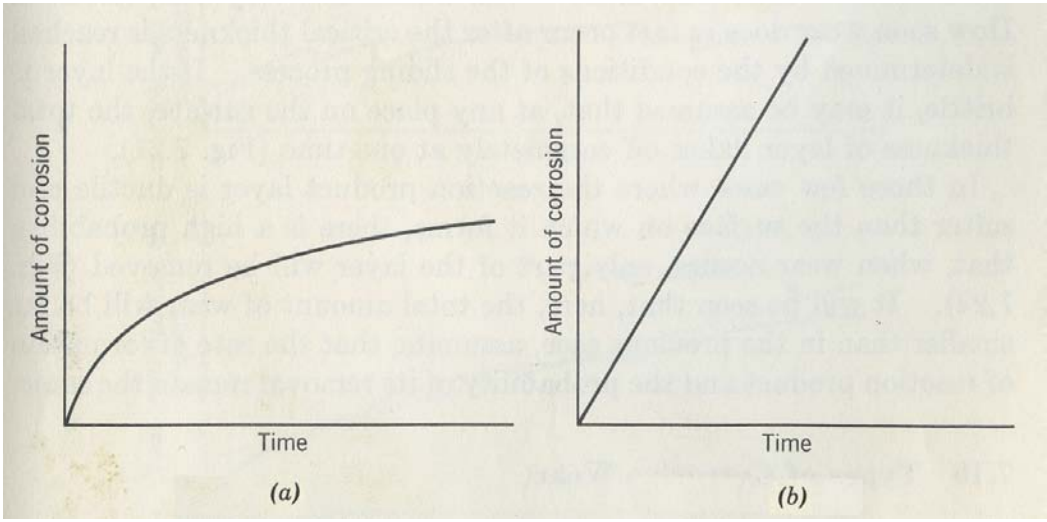

Fig. 1-11. Corrosion-time curve when (a) protective film is formed or (b) no protective film is formed [Ref. 1]

1.1.3 Testing methods for different types of wear

Since there are different wear types, various testing methods have been invented to evaluate the wear resistance of materials under different wearing conditions; some of the methods are already standardized to ensure the comparability of different tests.

The commonly utilized apparatus are pin-on-disc rig, dry sand rubber wheel rig, and slurry test rig and air-jet solid-particle erosion tester. These apparatuses are schematically shown in Fig 1-12. The first tribometer, the pin-on-disc tester is convenient to operate, and the wear tests reported in this thesis are all performed on this tester. During the test, a ceramic ball or a steel ball is used as the pin end and the material being tested as the disc; they work together as a wear pair. As annotated in Fig 1-12 (a), F is the normal load applied on the pin, r is the radius of pin or ball, R is the radius of the wear track and ω is the rotation velocity of the disc. For wear tests reported in this thesis, all testing conditions were the same, among which normal load was 10 N, wear track radius was 1 mm, the pinning ball was a Si_3N_4 ball with its diameter equal to 6 mm, linear speed of rotation was 0.5 cm/s and the total laps of rotation was 10,000. After the pin-on-disc test, the width of the wear track was measured and the volume loss of material was calculated accordingly.

The dry sand rubber wheel rig is usually used for low-stress abrasive wear tests. During the test, specimen is pushed against the rubber wheel vertically by loading

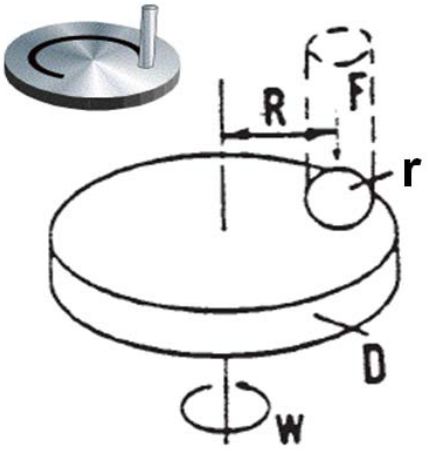

(a) Pin-on-disc rig [Ref. 10]

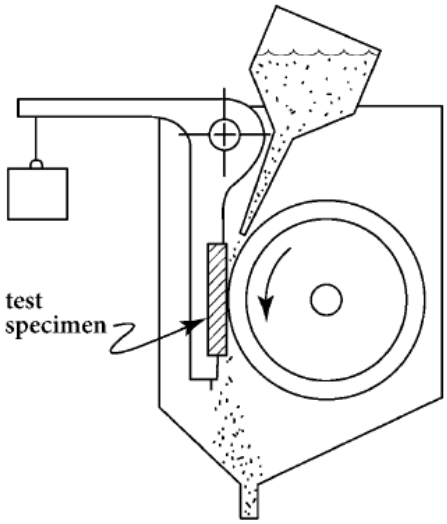

(b) Dry sand rubber wheel rig [Ref. 11]

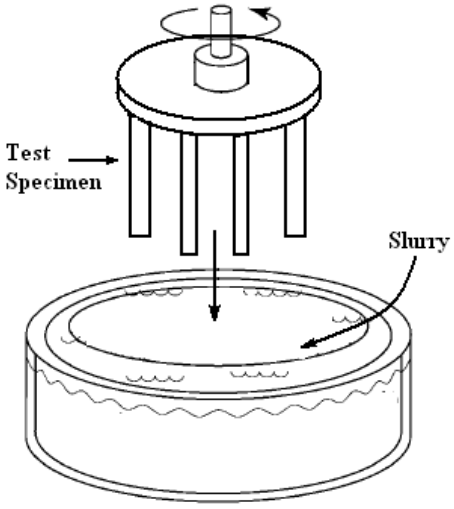

(c) Slurry test rig

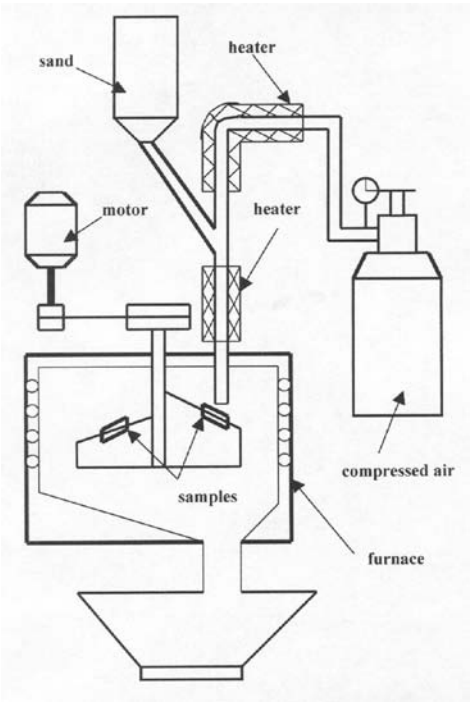

(d) High-T air-jet erosion tester

Fig. 1-12. Schemes of different tribometers

at the end of the horizontal arm of the crank as depicted in Fig 1-12 (b), and hard particles (usually sand of different sizes, hardness and shapes) are fed into the gap between the specimen and the rubber wheel. The rotation velocity and rotation direction of the rubber wheel are also variables so that the abrasive wear tests can be conducted under different but controlled conditions.

The slurry test rig is designed for erosion wear or erosion/corrosion wear. A total number of four samples can be fastened on one holder which is connected to a motor spinning at different speeds. The concentration of particles, particle sizes, particle shapes, particle hardness in slurry and the pH value of the slurry can be adjusted. After determining the configurations, the specimens are immersed into the slurry and eroded when spinning.

The air-jet solid-particle erosion tester allows a sample attacked by sand particles travelling at high speeds, which may reach 100m/s. This tester helps to evaluate the resistance of materials to wear involving impact force and to obtain information related to fracture toughness. The tester can run tests at elevated temperature up to 1000^{o}C.

For the latter three test protocols, the weight loss is often recorded first and volume loss is converted from weight loss when the materials being compared are not of the same density.

1.2 Properties of materials related to wear and pseudo-elasticity

In this thesis, there are mainly four kinds of materials involved, which are tungsten carbide (WC), cobalt (Co), titanium carbide (TiC) and titanium nickel (TiNi) alloy.

1.2.1 Tungsten carbide-cobalt (WC-Co) composite materials

In many cases, wear-resistant materials consist of hard carbides and a metal matrix phase. WC-Co composite is one of remarkable representatives. The application of WC-Co composite materials was initiated in the early 20th century; it consists of hard WC particles and a ductile Co matrix. This composite exhibits high wear resistance in many situations [12]. Apart from this, WC-Co composite also possesses a low production cost compared to other tribological materials. Over decades of development, this material is widely used in cutting tools, drilling, mining equipment and valves in erosive environment [13]. Fig. 1-13 vividly demonstrates the usage of cemented WC-Co composite.

The high wear resistance results from the WC particles bearing the wearing force, while the ductile Co matrix which is compatible with tungsten carbide provides considerable toughness, and toughness is highly desired when the material is subjected to wear involving impact. The prevalence of WC-Co composite material can be attributed to the following reasons. Firstly, during conventional manufacturing of the composite, sintering or arc-melting for instance, there might be inter-alloying between cobalt and carbide [15], which provides strong bonding

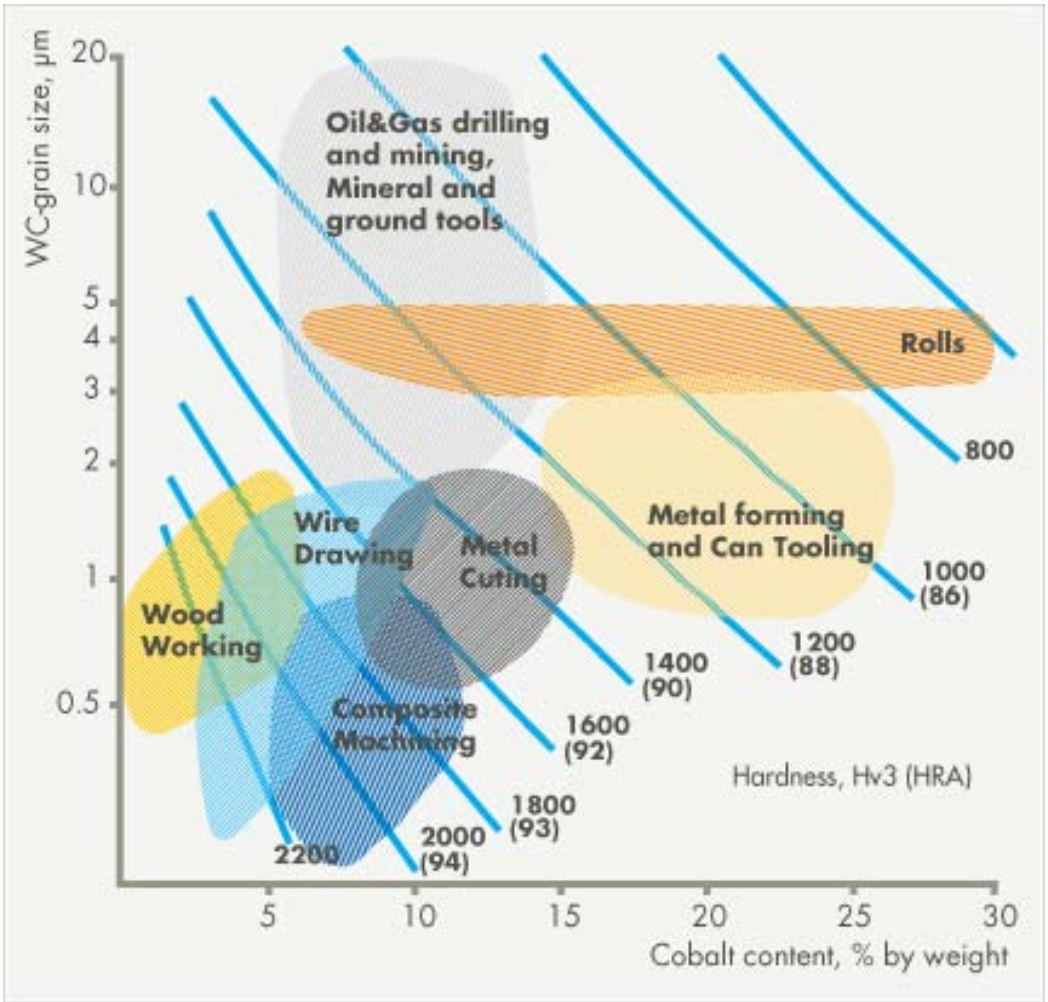

Fig. 1-13. The application range of cemented WC-Co composite [Ref. 14]

of the interfaces within the composite; secondly, during cooling of the manufacturing process, cobalt contracts more than tungsten carbide, which leads to compressive stress in WC grains. The compressive stress will reduce the possibility of brittle fracture for WC grains and lower the chance of deformation of Co matrix [16]; thirdly, the fcc-hcp transition of cobalt can occur during deformation, which further renders ductility to the binder [16-17].

Although WC-Co composite is popular in tribological application, its usage is still limited, e.g., by its brittleness [18] when the volume fraction of WC is high or low wear resistance of the metal matrix when the volume fraction of Co matrix is increased. M.G. Gee et al [19] showed that the main failure mechanism of cemented WC-Co under wear circumstances is due to removal of binder metal Co and accumulation of plastic deformation in grains of WC. Therefore, a lot of effort has been made to modify the properties of WC-Co. A dual WC-Co composite was developed to increase the fracture toughness [20], WC-Co composite with finer grains and nano-structured WC-Co composite have drawn considerable attention in studies related to the wear performance or the mechanical properties of the material [21-23], microwave sintering was compared with conventional sintering method [24] and etc., all of these endeavor has one purpose in common, which is improving the fracture toughness of WC-Co composites while maintaining the wear resistance of the metal matrix at an acceptable level.

1.2.2 Titanium carbide (TiC)

Similar to tungsten carbide, titanium carbide is often used as a reinforcing phase for wear-resistant materials in forms of composites or cements. This carbide is even harder than tungsten carbide. Besides, TiC-based composites are lighter and generally possess higher oxidation resistance and lower friction coefficient when compared with WC-base composites [25]. Apart from these, due to its chemical

inertness [26], TiC-based cermets or coatings have applications in extreme environment such as space where ball bearing and fretting joints are involved [27]. However, TiC-based cermets are more costly than WC-Co composites, so it is not utilized as widely as WC-Co composites.

TiC-based cermets follow the general trend of conventional tribological materials that the wear rate decreases as the hardness increases, as illustrated in Fig. 1-14 in which T_1 represents a TiC-16wt%Ni-4wt%Mo, T_2 represents TiC-32wt%Ni-8wt%Mo, and T_3 represents TiC-40wt%Ni-1wt%Mo.

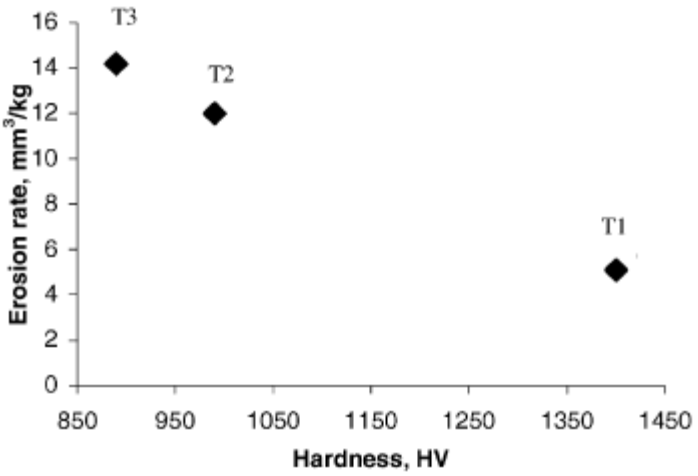

Fig. 1-14. Erosive wear rate of the TiC cermets versus their hardness [Ref. 26]

In another study concerning Fe-TiC composites under dry sliding, it is found that the wear rate and friction coefficient decrease with the increase in TiC content [28]. Although WC or TiC reinforced composites prove to be exceptional representative of tribological materials, they share one disadvantage in common that it is difficult to improve wear resistance and toughness at the same time.

1.2.3 Titanium nickel (TiNi) alloy

In order to increase the fracture toughness of WC-Co composite but at a less cost of wear resistance and hardness, pseudo-elastic TiNi alloy is introduced into the system. Research in the past three decades proved that pseudo-elastic TiNi possesses high wear-resistance when the composition of alloy is near equi-atomic [29]. According to Shida and Sugimoto [30], the TiNi alloy demonstrated remarkable resistance when the composition of the alloy was in the range of Ti-55wt%Ni to Ti-56.5wt%Ni, in which the TiNi alloy takes on super-elasticity or namely, pseudo-elasticity. The phenomenon of pseudo-elasticity is attributed to reversible phase transformations in TiNi alloy [31, 32], as illustrated in Fig.1-15.

In a sliding wear test conducted by C. Zhang and Z.N. Farhat [33], TiNi alloy with the composition of Ti-53~56wt%Ni was compared with Ti and Ni metals, as shown in Fig. 1-16. The condition of the test included a speed of 50 m/min and a load of 40N. The wear rate of TiNi alloy was considerably lower than that of Ti or Ni metal. Since Ni-based composite is conventional in tribology, it is reasonable to expect that TiNi alloy can be a better matrix material for tribo-composites than Ni.

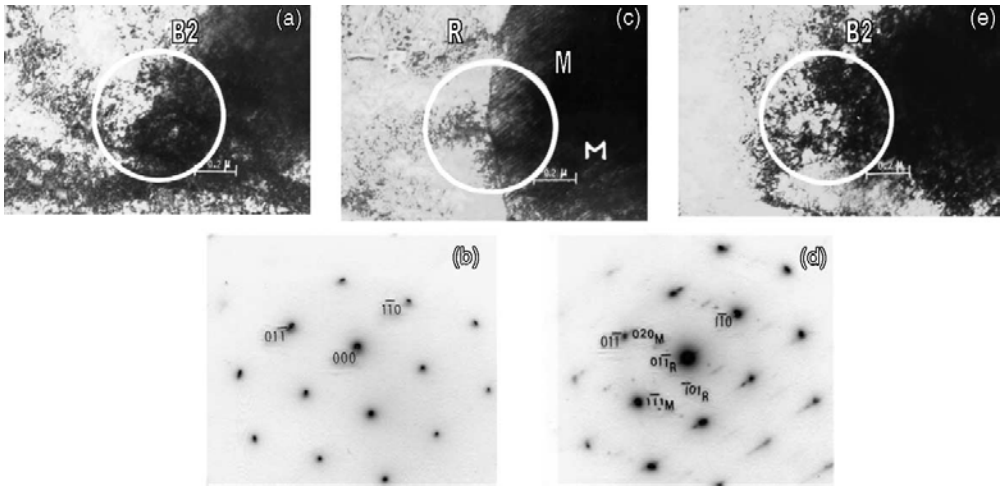

Fig. 1-15. Reversible phase transformations induced by applied tensile stress: (a) a selected field in stress-free condition and (b) corresponding diffraction pattern; (c) M and R phases were induced by stress, and (d) corresponding diffraction pattern; (e) M and R phases transformed back to B2 when stress was removed [Ref. 32].

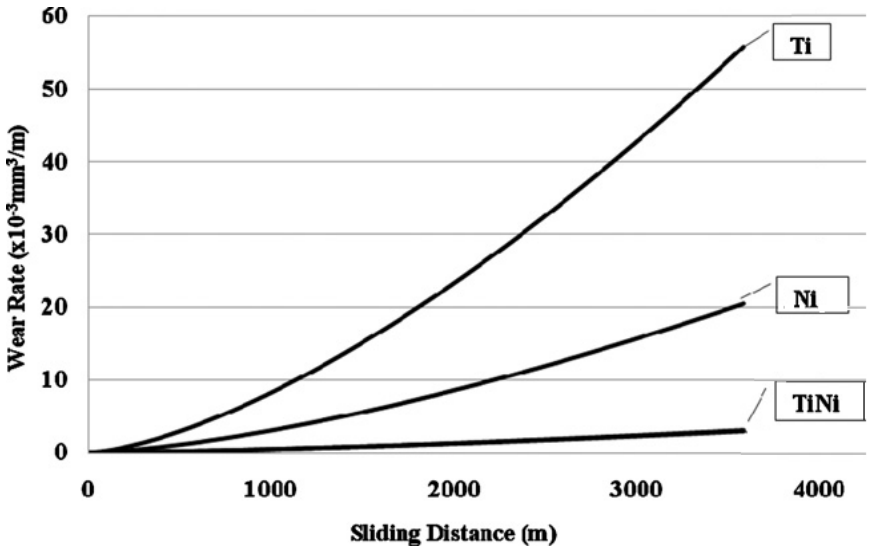

Fig. 1-16. Wear rate versus sliding distance of TiNi alloy, Ti and Ni metals [Ref. 33]

When compared to 2Cr13 steel, the alloy with a composition of Ti-50.3at% Ni again demonstrated higher wear resistance, as depicted in Fig. 1-17 [34]. Moreover, it should be emphasized that the hardness of this TiNi alloy (ranges from 200 to 500 Hv) is lower than that of 2Cr13 steel (610 Hv). This phenomenon is unusual in comparison with conventional tribo-materials, because it is commonly assumed that the wear resistance of a material will rise with higher hardness. So the TiNi alloy may suggest an alternative approach to boost the ductility and toughness of carbides reinforced materials without compromising the wear resistance.

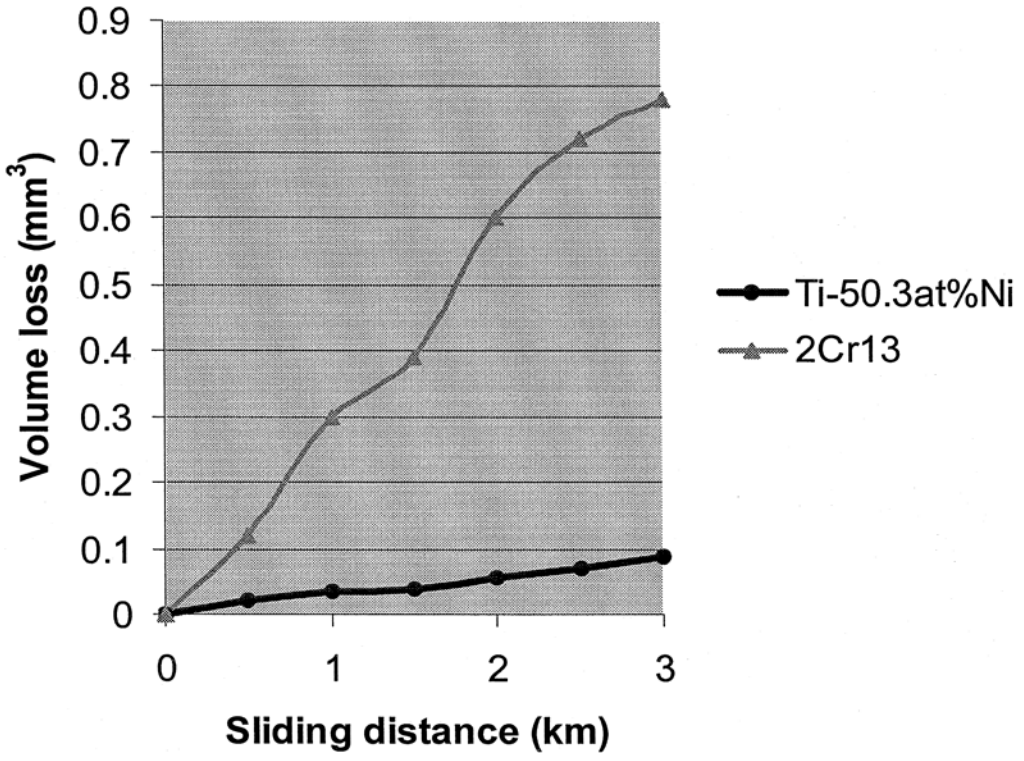

Fig. 1-17. Volume wear loss of Ti-50.3at% Ni alloy and 2Cr13 steel [Ref. 34]

1.3 Objective of this study

As mentioned above, this study focuses on the modification of commercial WC-Co composite which is extensively used for tribological applications. In most cases, compromise of hardness has to be made when toughness of the material is promoted by various approaches. In this study, a pseudo-elasticity TiNi alloy phase is added to the relatively ductile but less wear-resistant Co matrix for enhanced wear resistance of WC-Co composite while maintaining or improving the overall toughness.

Furthermore, direct use of TiNi alloy as a matrix for WC has also been investigated. WC-Co, WC-TiNi and TiC-TiNi composites were prepared, their wear resistances were evaluated and compared. For WC-TiNi, since Co is replaced by TiNi, one may find out whether TiNi alloy is an appropriate candidate matrix for WC in terms of its compatibility with WC; TiC-TiNi composite was expected to possess better interface bonding between hard particles and matrix when compared with the WC-TiNi composite.

1.4 Brief on following chapters

Chapter 2 describes the experimental techniques used in this study for all the processes from sample preparation to microstructure characterization.

Chapter 3 is the full text of a published paper with the tile of “Enhancing the wear resistance of sintered WC-Co composite by adding pseudo-elastic TiNi

constituent". This paper reports a study regarding TiNi alloy's influence on the wear resistance of WC-Co composites. To ensure good sinterability, high cobalt content (60wt %) in the composite is used despite the fact that it is not common in commercial applications. It was demonstrated that markedly enhanced wear resistance was achieved when a proper amount of TiNi powder was added to the WC-Co composite. The sintered WC-Co-TiNi specimens were analyzed using the X-ray diffraction technique (XRD) and scanning electron microscopy (SEM). It was observed that a certain degree of decomposition of the added TiNi occurred during the sintering process. In order to clarify the mechanism responsible for the improvement to the wear resistance, local mechanical properties of different domains, including hardness, Young's modulus and the ratio (η) of elastic deformation energy to the total deformation energy were evaluated using a micro-indenter. Based on the microstructure characteristics and micro-mechanical properties of different domains, efforts are made to understand the role that the added TiNi powder played in enhancing the wear resistance of the WC-Co composite.

Chapter 4 reports a preliminary study represented in a potential paper entitled "Comparison of the wear resistances of WC-Co, WC-TiNi and TiC-TiNi composites". In order to determine whether TiNi alloy matrix composites possess comparable tribological property to WC-Co composite, three different composites, WC-Co, WC-TiNi and TiC-TiNi with the same volume fraction (60%) of metal matrix were sintered using a hot isostatic pressing (HIP) process and their wear tracks were tested with pin-on-disk technique for preliminary comparison; results

showed that TiC-TiNi composite presented the narrowest wear track (corresponding to the highest wear resistance) while WC-Co composite had the widest one. Meanwhile, according to the fact that commercially-used tribological materials commonly attempt to use a decreased fraction of metal matrix, these three composites with lower volume fractions (43% and 20%) of metal matrix were also studied in the same way, among which WC-Co composites revealed the narrowest wear tracks.

Chapter 5 includes the summary of this thesis, which outlines the findings and the problems in this study, also the discussion of possible work to be done in the future.

Reference

[1] Ernest Rabinowicz, Friction and wear of materials, A Wiley-Interscience Publication, 1965

[2] A.R. Lansdown and A.L. Price, Materials to resist wear - a guide to their selection and use, Pergamon Materials Engineering Practice, 1986,

[3] J.A. Williams, Wear and wear particles - some fundamentals, Tribology International 38 (2005) 863-870

[4] A.D. Sarkar, Wear of metals, Oxford, New York, Pergamon Press, 1976

[5] J. Halling, Introduction to tribology, Wykeham Engineering and Technology Series, 1976

[6] K.C. Ludema, Friction, Wear, Lubrication: A Textbook in Tribology, CRC Press, 1996

[7] R.M. Davis, The determination of static and dynamic yield stresses using a steel ball, Proc. Roy, Soc., A 197 (1949) 416-432

[8] N.P. Suh, Tribophysics, Englewood Cliffs NJ: Prentice-Hall, 1986

[9] B. Pugh, Friction and wear: a tribology text for students, London, Newnes-Butterworths, 1973

[10] ASTM Standard G 99-05, Standard Test Method for Wear Testing with a Pin-on-Disk Apparatus, Annual Book of ASTM Standards, vol. 03.02, 2005

[11] Kenneth G. Budinski, Guide to Friction, Wear, and Erosion Testing: (MNL 56), ASTM International, 2007

[12] H.E. Exner and J. Gurland, Powder Metall., 13 (1970) 1146

[13] D.K. Shetty, I.G. Wright, P.N. Mincer and A.H. Clauer, Indentation fracture of WC-Co cermets, Journal of Materials Science, 20 (1985) 1873-1882

[14] Sandvik hard materials group, Catalogue of Cemented Carbide, 2005

[15] Dinesh Agrawal, A.J. Papworth, J. Cheng, H. Jain and D.B. Williams, Microstructural examination by TEM of WC-Co composites prepared by

conventional and microwave process, Proceedings of 15th international plansee seminar, 2 (2001) 677-684

[16] J. Larsen-Basse Binder extrusion in sliding wear of WC-Co alloys, Wear 105 (1985) 247–256

[17] Gopal S. Upadhyaya, Cemented tungsten carbides: production, properties, and testing, Noyes Publications, 1998

[18] J.L. Chermant and F. Osterstock, Fracture toughness and fracture of WC-Co composites, Journal of Materials Science, 11 (1976) 1939-1951

[19] M.G. Gee, A.J. Gant, B. Roebuck, Wear mechanisms in abrasion and erosion of WC-Co and related hardmetals, Wear, 263 (2007) 137-148

[20] Z. Fang, G. Lockwood and A. Griffo, A dual composite of WC-Co, Metallurgical and Materials Transactions A 30 (1999) 3231–3238

[21] W.D. Schubert, H. Neumeister, G. Kinger, B. Lux, Hardness to toughness relationship of fine-grained WC-Co hardmetals, International Journal of Refractory Metals and Hard Materials, 16 (1998) 133-142

[22] C. Allen, M. Sheen, J. Williams and V.A. Pugsley, The wear of ultrafine WC-Co hard metals, 250 (2001) 604-610

[23] K. Jia, T.E. Fischer, B. Gallois, Microstructure, hardness and toughness of nanostructured and conventional WC-Co composites, NanoStructured Materials, 10 (1998) 875–891

[24] E. Breval, J.P. Cheng, D.K. Agrawal, P. Gigl, M. Dennis, R. Roy and A.J. Papworth, Comparison between microwave and conventional sintering of WC-Co composites, Materials Science and Engineering: A, 391 (2005) 285-295

[25] Jakob Kübarsepp, Heinrich Klaasen, Jüri Pirso, Behaviour of TiC-base cermets in different wear conditions, Wear, 249 (2001) 229-234

[26] I. Hussainova, Effect of microstructure on the erosive wear of titanium carbide-based cermets, Wear, 255 (2003) 121-128

[27] H.J. Boving, H.E. Hintermann, Wear-resistant hard titanium carbide coatings for space applications, 23 (1990) 129-133

[28] V.K. Rai, R. Srivastava, S.K. Nath, S. Ray, Wear in cast titanium carbide reinforced ferrous composites under dry sliding, Wear 231 (1999) 265–271

[29] H.Z. Ye, D.Y. Li and R.L Eadie, Improvement in wear resistance of TiNi-based composites by hot isostatic pressing, Materials Science and Engineering: A, 329-331 (2002) 750-755

[30] Y. Shida and Y. Sugimoto, Water jet erosion behaviour of Ti-Ni binary alloys, Wear, 146 (1991) 219-218

[31] Q. Chen and D.Y. Li, A computational study of the improvement in wear resistance of a pseudoelastic TiNi matrix composite achieved by adding TiN nanoparticles, Smart Materials and Structures, 16 (2007) S63-S70

[32] D.Y. Li, Development of novel tribo composites with TiNi shape memory alloy matrix, Wear 255 (2003) 617–628

[33] C. Zhang, Z.N. Farhat, Sliding wear of superelastic TiNi alloy, Wear, 267 (2009) 394-400

[34] D.Y. Li and Rong Liu, The mechanism responsible for high wear resistance of Pseudo-elastic TiNi alloy—a novel tribo-material, Wear, 225-229 (1999) 777-783

Chapter 2

Experimental techniques

Chapter 2 - Experimental techniques

2.1 Sample preparation

Powder metallurgy method is the main technique applied in preparing the samples. Powders of carbides (tungsten carbide or titanium carbide), cobalt, and titanium nickel were weighed according to designated compositions for different experiments, and then mixed using the dry ball mill method for 2 hours, followed by cold pressing into green pellets with a hydraulic press. The compacted green pellets had a diameter of 8 mm with their height around 4 mm. Thereafter, the green specimens are moved to alumina crucibles and sintered in the chamber of a hot isostatic pressing (HIP) machine (HP630, AIP, USA) in an argon atmosphere. The sintering processes were carried out under the following condition that was commonly used in this study: temperature = 1500^{o}C and pressure = 4000 psi with a holding duration of 3 hours.

This sintering temperature was selected according to the pseudo-binary phase diagram constructed by Grüter [1], as shown in Fig. 2-1. In the figure, β phase refers to Co and η stands for Co_6W_6C or Co_3W_3C. Since liquid phase is desirable for removing open pores and pressurizing closed pores of the green samples, the final sintering temperature was chosen to be 1500 ^{o}C.

Fig. 2-2 shows the HIP machine and the appearance of control panel which configures everything of the HIP system in the software.

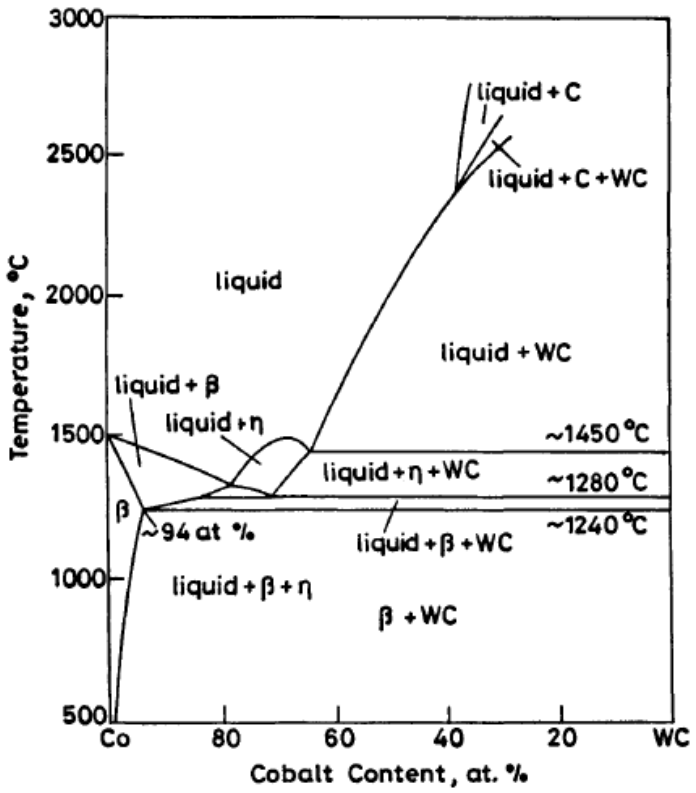

Fig. 2-1. Pseudo-binary phase diagram for WC-Co system

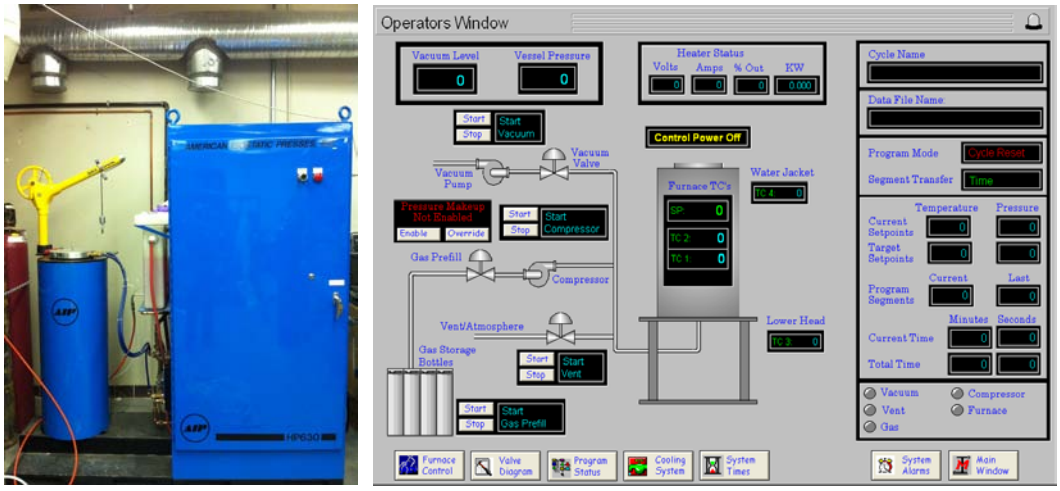

Fig. 2-2. A hot isostatic pressing system and software interface of the hot isostatic pressing system

2.2 Wear testing

The sintered samples were ground on a series of SiC papers with gradually increasing grit sizes and polished with diamond paste of one micro diameter for a flat and smooth surface. The polished samples were then loaded on a tribometer (CSEM instruments) for wear tests (see Fig. 2-3). A Si_3N_4 ball (diameter = 6 mm) was pushed against the sample under a vertical load of 10N and the radius of the wear track was adjusted to be 1 mm. After a total of 10000 rotation laps with a linear speed of 0.5cm/s, the sample was observed under a Leica microscope (Type: 090-135003) as shown in Fig. 2-4 and the width of the wear track was measured with Image Pro Plus 6.1; or a Zeiss Axio CSM 700 confocal microscope (see Fig. 2-5) was employed for more precise measurements. With the idea of point-by-point illumination, elimination of unwanted fluorescence by constraining the light source and rejection of out-of-focus light by a screen with pinhole, this microscope was capable of providing sharper images with less background haze than the conventional microscope, and it could also detect the height information on the vertical orientation (the direction that is perpendicular to the surface) of the sample since the working distance was adjusted during observation to ensure every region of the specimen is in focus [2]. The profiles of the wear tracks were depicted with and the volume losses were integrated with Origin 8.5.

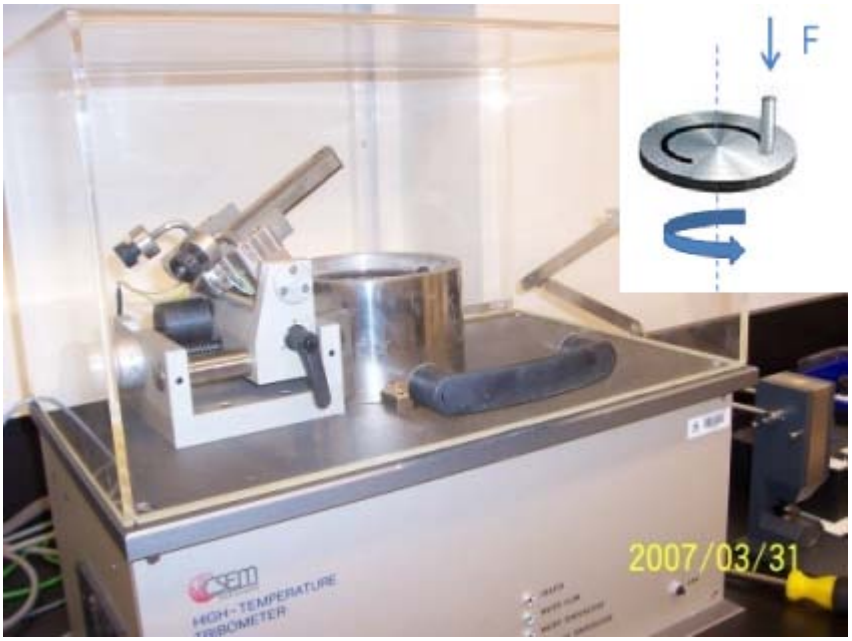

Fig. 2-3 A pin-on-disc tester for the present wear tests

Fig. 2-4. Leica microscope for observing wear tracks

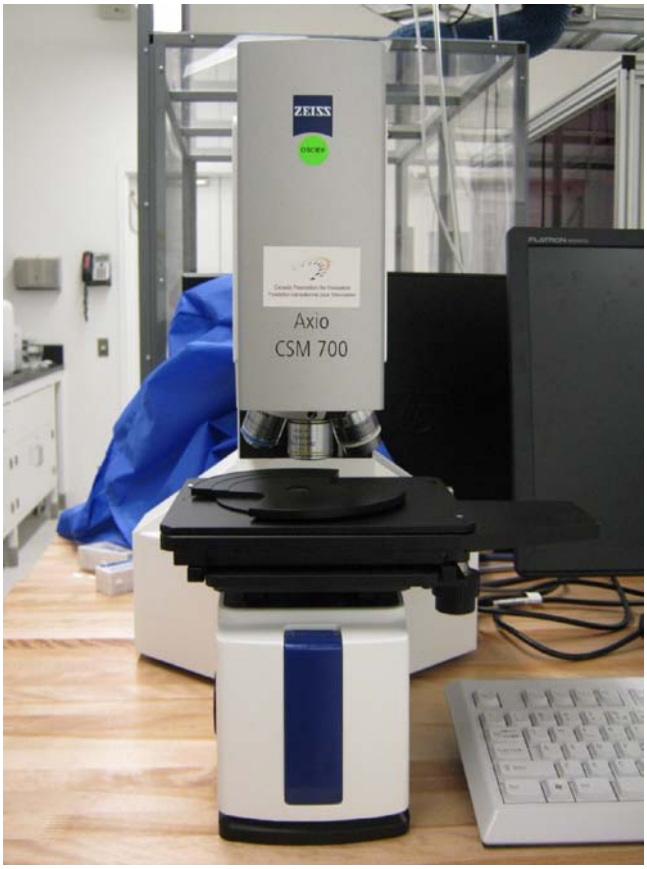

Fig. 2-5. Zeiss confocal microscope

2.3 Characterization of samples

Besides the wear tests, the macro- and micro-hardness tests of samples were conducted either on Mitutoyo AVK-C1 hardness tester (Fig. 2-6) or on a micro-indentation hardness tester from Fisher (Fig. 2-8). Vickers hardness was obtained from the Mitutoyo AVK-C1 hardness tester by measuring the length of the two diagonals of the resultant indentation.

Equation 2-1 gives an approximate approach to calculate the Vickers hardness.

$$Hv=1.854 \cdot F/d^2 \quad (2\text{-}1)$$

where F is load in kgf, d is arithmetic mean of the two diagonals, d_1 and d_2 in mm, as d_1 and d_2 are shown in Fig. 2-7 [3].

Fig. 2-6. Mitutoyo AVK-C1 hardness tester

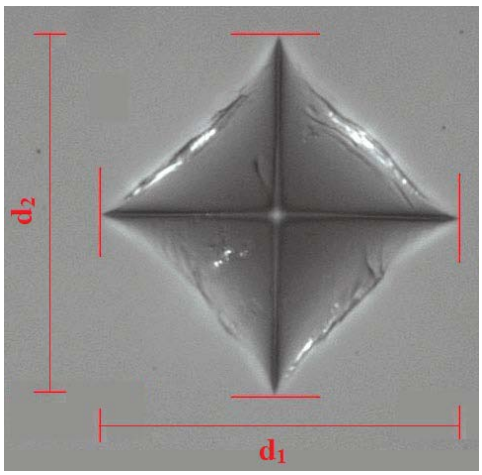

Fig. 2-7. Appearance of Vickers indentation [Ref. 2]

From micro-indentation, not only the hardness of certain phase is given, the ratio (η value) of elastic deformation energy (W_e) to the total deformation energy (W_{tot}) is given provided as well. A typical curve of load versus indentation depth in the indentation test is illustrated in Fig. 2-9a, in which W_e is the area under the unloading part of the curve (see Fig. 2-9b) and W_{tot} is the area under the loading part of the curve (see Fig. 2-9c).

Fig. 2-8. A micro-indentation system (Fischerscope H100C)

For analysis of the reaction during sintering, the X-ray diffraction (XRD) technique was applied to identify the phases in samples. The morphology and the microstructure of samples were observed or analysed with scanning electron microscopy (SEM) and the energy dispersive spectroscopy (EDS).

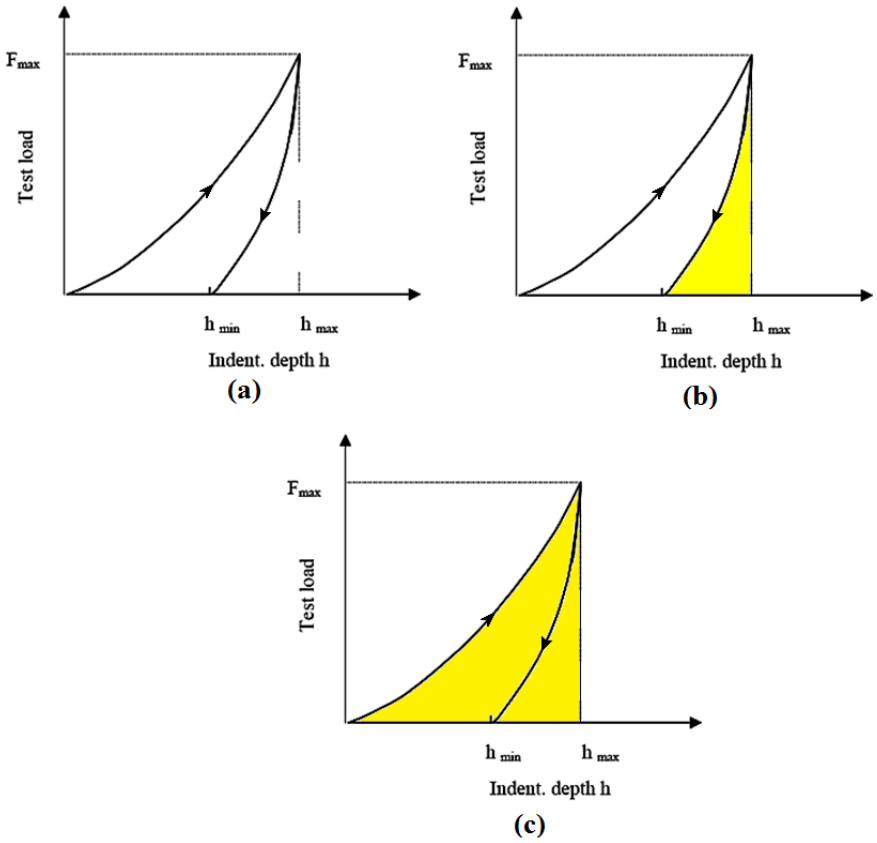

Fig. 2-9. Indentation curve and demonstration of η value calculation

Reference

[1] M. Grüter, Untersuchungen in den systemen Co-C, Co-W und Co-WC, Münster, F.R.G., 1959

[2] V. Prasad, D. Semwogerere, E.R. Weeks, Confocal microscopy of colloids, J. Phys.: Cond. Mat., 19 (2007) 113102

[3] ASTM Standard E 384-11, Standard Test Method for Knoop and Vickers Hardness of Materials, Annual Book of ASTM Standards, vol. 03.01, 2011

Chapter 3

Enhancing the wear resistance of WC-Co composites with a pseudoelastic TiNi phase

Chapter 3 - The benefit of TiNi ally to the wear resistance of WC-Co composite

3.1 Introduction

The use of commercial WC-Co as a wear-resistant material can be dated back to 1920's [1]. WC-reinforcing Co composites are widely used in forms of bulk, plates, hardfacing overlay and coatings in various industrial sectors [2-6] for, e.g., cutting, drilling, and moulding, etc., where the wear resistance is demanded. The hard WC plays a main role to withstand the wearing force while the ductile metallic matrix helps to absorb impact energy and accommodate large deformation as well as acts as a binder to retain the hard carbides. Co has relatively high compatibility with WC, leading to strong interfacial bonding with the carbide. Such a combination of hard reinforcements and a ductile matrix provides balanced hardness and toughness. However, in many cases, the ductile matrix is preferentially attacked by wear, leading to pull-off of the hard carbides. Reducing the volume fraction of the ductile matrix may not always be an effective approach, since this reduces the toughness of the composite, making it less durable particularly during wear processes especially when impact force is involved. Selecting different metallic materials for the matrix is a logical approach. However, if a harder matrix is used, the composite will also lose its toughness and thus the capabilities of absorbing impact energy and accommodating deformation. Besides, since the bonding between of the carbide and the matrix must be strong, choices of appropriate matrix material are limited.

The fracture toughness is a crucial parameter, which has attracted long-term attention [7]. Efforts have been made to improve WC-Co composites by, e.g., adding Mo and Nb particles [8]. Using nano-structured WC-Co is another approach to obtain improved balance between hardness and toughness [9]. Adding NbC to WC-Co cements also showed some benefits [10]. There are still other approaches, e.g., a proposed dual WC-Co composite with WC-Co granules embedded in Co matrix, boosted the fracture toughness [11]. However, since hardness and toughness cannot be increased simultaneously with conventional materials technologies, it is hard to expect that the wear resistance can be considerably increased by modifying the hardness of the matrix or changing the volume fraction of the matrix.

In this study, we explore an alternative approach to improve WC/Co composites by incorporating a pseudoelastic or rubber-like metallic phase into the Co matrix. A typical pseudoelastic material is the near equi-atomic TiNi shape memory alloy with a thermo-elastic phase transformation. This pseudoelastic (PE) alloy is flexible but possesses excellent wear resistance due to the fact that the pseudo-elasticity helps to accommodate large-scale strain reversibly and dissipate impact energy effectively, resulting in excellent wear resistance in different wear modes [12,13]. TiNi alloy demonstrates remarkable resistance when the composition of the alloy is in the range from Ti-55wt%Ni to Ti-56.5wt%Ni [14, 15], in which the TiNi alloy behaves like a metal rubber, known as the pseudo-elasticity as mentioned earlier, which results from a thermo-elastic phase transformation of TiNi alloy [12, 13]. Fig.3-1 illustrates a representative stress – strain curve of a

pseudoelastic TiNi alloy.

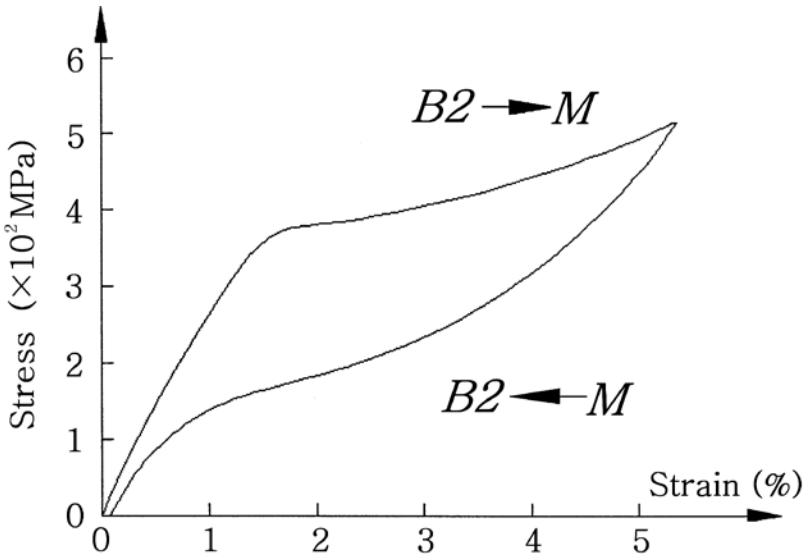

Fig. 3-1. A representative tensile stress-strain curve showing the pseudo-elasticity of a nominal Ti-51 at% Ni alloy at room temperature

As shown, at a certain stress level, the alloy is “yielded”, which is caused by the initiation of a phase transformation from a parent phase (B2) to a martensitic phase [12]. This phase transformation is reversible and can be induced by stress. The large strain can be recovered when the applied stress is removed. It should be mentioned that the stress-induced phase transformation exists when temperature is above the phase transformation temperature [12, 13, 16]. When temperature is below the phase transformation temperature, the alloy is in a martensitic state. Stress can induce re-arrangement of martensitic variants, which may lead to the pseudoelastic behaviour as well. The pseudo-elasticity makes the rubber-like alloy able to accommodate deformation resulting from the wearing force with

minimized damage. Besides, the specific volume of martensite is about 4% larger than that of the B2 phase [17, 18]; this may result in compression in the alloy that is resistant to crack propagation.

The pseudoelastic alloy can be used as matrix for composites for enhanced wear resistance. This has been confirmed by previous studies on TiC/TiNi composites [13]. If the pseudoelastic alloy is used as a second phase in the Co matrix, we may expect improved wear resistance with retained strong interfacial bonding between the metallic matrix and WC reinforcements. Confirming this hypothesis through investigating TiNi-added WC/Co composites is the main objective of this study.

In this preliminary study, WC-60%Co composite was used as a sample composite for modification with TiNi. Selection of the high fraction of Co was to ensure that there was enough metallic matrix, which facilitated the investigation of the effect of added TiNi on the improvement to the matrix and consequently the overall wear resistance.

3.2 Experimental Details

3.2.1. Sample preparation

Mixed powder of WC and Co was provided by Alfa Aesar (WC:Co = 94:6 wt%, 99%, metal basis, -325 mesh). Co powder was also purchased from the same supplier in order to change the fraction of Co matrix in the planned WC-Co-TiNi composites (99.8%, metal basis, -100+325 mesh, spherical). Pseudoelastic TiNi

alloy powder was provided by SAES smart materials (-80+100 mesh) with the composition in the range from Ti-55 wt%Ni to Ti-56.5 wt%Ni. The martensitic transformation temperature (Ms) depends on the ratio of Ti to Ni, and effective pseudo-elasticity may exist at temperature up to about 30 degrees above Ms [16]. For the present composition range, the maximum Ms is about 50^{o}C, implying that the TiNi powder may possess pseudo-elasticity or partial pseudo-elasticity from about 80^{o}C down to a temperature below -100^{o}C (depending on the composition of individual TiNi particles).

Powders of different constituents were weighed and then mixed using a dry ball milling process. Samples having different compositions, listed in Table 3-1, were made. In this study, the weight ratio of WC to Co was at 40:60, and the weight percentage of TiNi alloy was varied in order to determine the influence of TiNi alloy on the wear resistance of the WC-Co composites.

Table 3-1. Fractions of mixed powders for different samples

	wt%	
Sample No.	TiNi	WC-60 wt%Co
1	0%	100%
2	5%	95%
3	10%	90%
4	15%	85%
5	20%	80%
6	25%	75%
7	30%	70%

Samples with mixed powders were pressed using a MP15 laboratory pellet press (Across International Company) under a pressure of 8 MPa for 5 minutes; each green sample was weighed approximately 1.2 grams with a thickness of 3mm and a diameter of 8mm. The green samples were then sintered using a hot isostatic pressing (HIP) machine (HP630, AIP, USA). The sintering scheme is set as follows: evacuate the furnace chamber to 0.250 torr and fill it with Ar to 20 psi for 2-3 times to ensure that a protective atmosphere was built; heat the furnace to 1500^{o}C at a heating rate of 12^{o}C/min while the pressure increases along with the rise of temperature; pressurize the furnace chamber to 4000 psi within 10 minutes; sinter the sample under a pressure of 4000 psi at 1500^{o}C in Ar for three hours. Fig.3-2 illustrates the sintering condition. This sintering process is based on a number of experimental trials; it may not be the optimal condition but should be effective for the present comparative study.

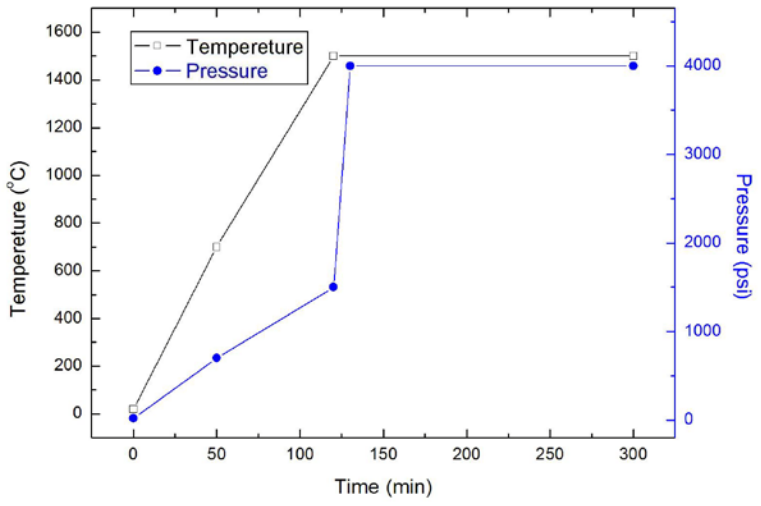

Fig. 3-2. Temperature and pressure vs. time for fabricating the WC-Co-TiNi composites

3.2.2. Characterization and Testing

Sintered samples were polished with SiC papers of different grits and finally polished with one-micron diamond paste. After etching, the polished samples were tested using a tribometer (CSEM instruments) at room temperature under a load of 10N at a speed of 0.5 cm/s for 10000 laps. The radius of the wear track was 1 mm and a Si_3N_4 ball (diameter = 6 mm) was used to abrade a sample surface. The wear track was examined under a Leica microscope (Type: 090-135003) and the width of the wear track was measured with Image Pro Plus 6.1. Fig. 3-3 shows a typical wear track on a sample of (WC-60Co)-10TiNi.

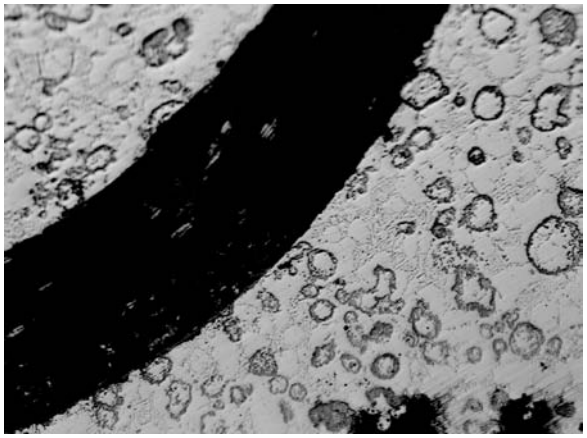

Fig. 3-3. A representative of wear track on a sample (WC-60Co)-10TiNi

The width of each wear track was determined by averaging values measured at eight different locations. If there is no significant wear on the ball as illustrated in Fig. 3-4 (a), the volume loss of a sample may be calculated as [19]

$$\text{Volume loss} = 2\pi R\,[r^2 \cdot \sin^{-1}(d/2r) - (d/4)\,(4r^2 - d^2)^{1/2}] \qquad (3\text{-}1)$$

where R = wear track radius; r = radius of pin ball, and d = wear track width.

The Vickers hardness of WC can get to 2200 when the after-sintering density is higher than 15.5 g/cm^3 [20], and that of Si_3N_4 ranges from 1500 to 2000 according to the information provided by Boca bearing company. For the composite of WC-Co, its hardness was expected to reduce due to the existence of Co as binder. Therefore the hardness of tested specimen and the pin ball may be comparable, and the pin ball i.e. a Si_3N_4 ball installed at the end of a rod to wear a target sample was also worn during the wear test as indicated in Fig. 3-4 (b). The larger the worn area of the pin ball, the more wear resistant is the target sample. Thus, the worn area of the pin ball may also be used as an approximate measure of the wear resistance of the target sample.

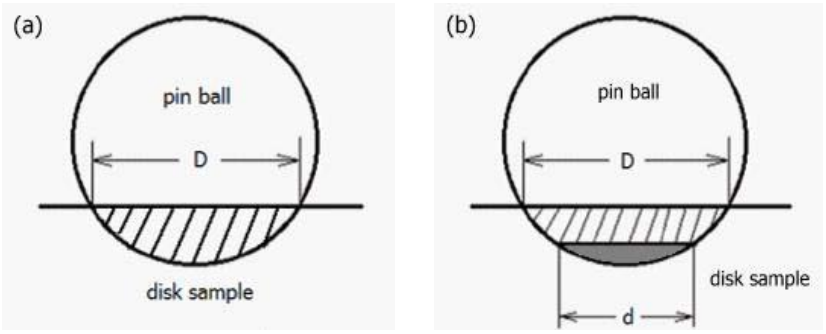

Fig. 3-4. Schematic of the cross-section area of a wear track (lined area), where D is the width of the wear track on a target specimen; d is the diameter of worn area of the pin ball (Si_3N_4); the grey area in (b) is the worn part on the ball

Micro-indentation tests were performed on different domains in the samples using a micro-indenter made by Fischer Technologies. In addition to hardness, η value

was also measured, which is the ratio of elastic deformation energy (the area under the unloading curve) to the total deformation energy (the area under the loading curve) [21]. This value is a measure of the elastic or pseudoelastic behavior of a material.

The phase state and microstructure of the sintered material were examined using the X-ray diffraction technique (XRD), scanning electron microscopy (SEM) and energy dispersive spectroscopy (EDS).

3.3. Results and discussion

3.3.1. Wear resistance and local mechanical behavior

The widths of wear tracks on different samples worn under a load of 10N at a linear speed of 0.5cm/s for 10000 laps were measured. Corresponding volume losses were estimated and are illustrated in Fig. 3-5. As shown, adding TiNi phase improved the wear resistance of the WC-60Co composite. The most effective amount of TiNi is 10 wt%. The wear track on WC-60Co is 23% wider than the wear track on the (WC-60Co)-10TiNi. The positive effect of the TiNi phase on the wear resistance decreased as the amount of added TiNi continuously increased as shown in Fig. 3-5.

The diameter of worn area of the pin ball was also measured for each wear test. Fig.6 illustrates the diameter versus the amount of added TiNi. As demonstrated, the diameter of the worn area on the pin ball increased initially and then decreased

as the amount of added TiNi was increased. The larger the worn area on the pin ball, the higher is the resistance of the target sample (WC-Co) to wear. The changes in the diameter of worn area on the pin ball are consistent with the changes in the width of wear track illustrated in Fig. 3-6.

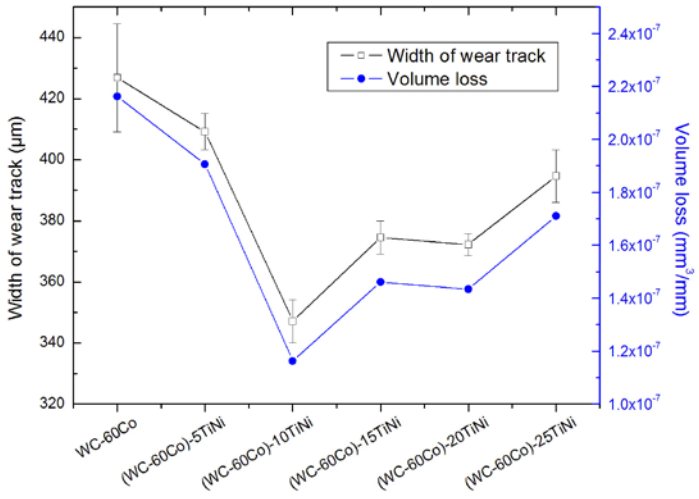

Fig. 3-5. The width of wear track and calculated volume loss of different samples worn under a load of 10N at a speed of 0.5cm/s for 10000 laps

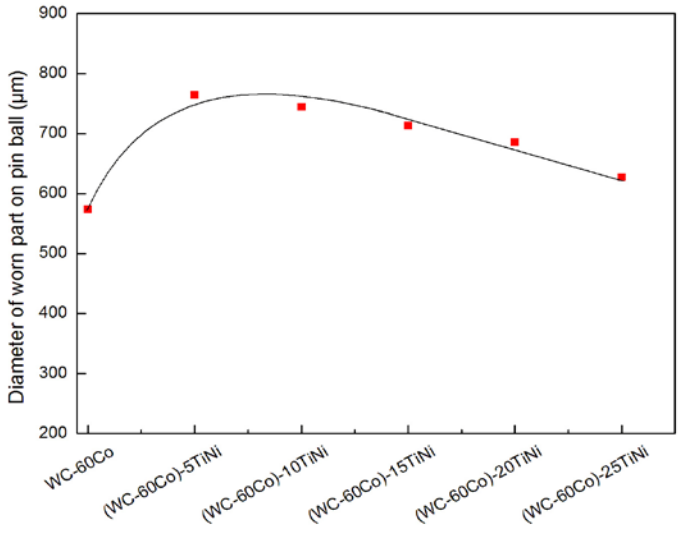

Fig. 3-6. Diameter of worn part on pin ball for different samples

Based on the wear track width (Fig. 3-5) and the size of worn area on the pin ball (Fig. 3-6), it appears that WC-60Co with added TiNi alloy in the range of 10 wt% resulted in the highest wear resistance.

In order to understand the improvement to the wear resistance by the addition of TiNi phase, local mechanical behavior of different domains in the samples was investigated using a micro-indenter. As shown in Fig. 3-7, micro-indentation was performed at different locations (marked as i_1, i_2, and etc.) on a (WC-60Co)-10TiNi sample. Measured hardness, maximum indentation depth (h_{max}) under a fixed load, Young's modulus, and the ratios (η values) of elastic deformation energy (W_e) to the total deformation energy (W_{tot}) are given in Table 3-2.

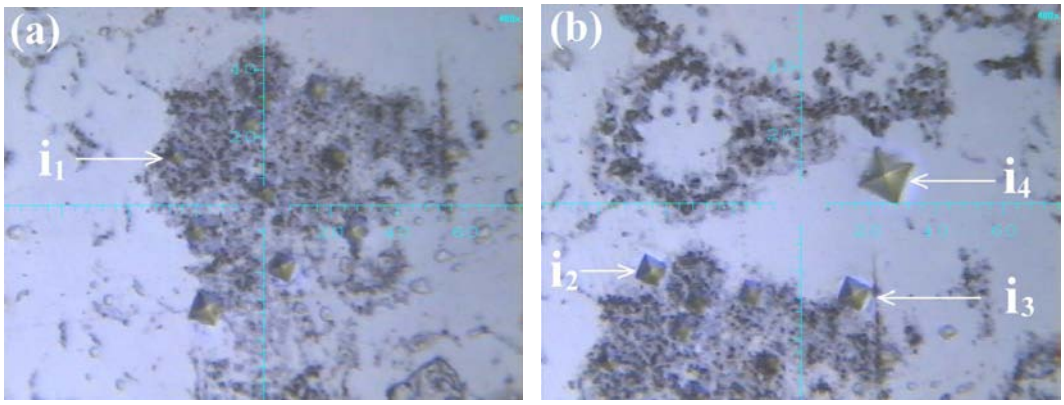

Fig. 3-7. Indentation tests on different domains. η value at spot i_1 is 49.53%

Table 3-2. Results of the micro-indentation on different domains tested under a maximum load of 500 mN

	W_e/W_{tot} (η, %)	Hv	h_{max} (μm)	E (GPa)
i_1	49.53	878.7	1.56	182.6
i_2	34.30	366.1	2.39	140.9
i_3	34.46	421.6	2.17	157.1
i_4	15.69	157.9	3.33	91.7

As shown in Table 3-2, η value of a dark zone marked by i_1 in the (WC-60Co)-10TiNi sample reached 49.53%. We also measured the η value of the TiNi matrix in a TiC-60 wt%TiNi composite and determined that the TiNi matrix had its η value at the same level. Since there is no decomposition of TiNi in the TiC-TiNi composite, this η value is an indication that the pseudoelastic TiNi phase was retained in the sintered WC-Co-TiNi composite. The dark zone marked with i_1 should be a cluster of TiNi phase. The zone marked with i_4 is the Co matrix, which is softer than the TiNi domain and its η value is much lower. Clearly, the TiNi phase is harder with the capability to accommodate deformation more elastically or reversibly according to its higher η value. These should lead to a considerable increase in the resistance to wear. The areas marked with i_2 and i_3 are zones between Co and the TiNi-containing zones where TiNi may react with Co; their mechanical properties have values between those of the TiNi and Co, as shown in Table 3-2.

3.3.2. Microstructures and compositions of different samples

When TiNi was added to the Co-matrix composite, TiNi and Co could react and this may consequently influence the performance of the composite. Thus, it is of importance to have the information on local microstructure and composition of the TiNi-added WC-Co composites. Microstructure and composition of (WC-60Co)-TiNi samples were characterized and determined. Fig. 3-8 illustrates microstructures of WC-60Co with different amounts of added TiNi. As shown, the WC-60Co had a eutectic microstructure. Adding TiNi caused changes in the morphology. It is worthy of emphasizing that some pores were observed in the samples. The sample of (WC-60Co)-10TiNi had fewer pores. The porosity and pore size increased with the amount of added TiNi. Such changes could be responsible for the deterioration of wear resistance as the TiNi amount was larger than 10 wt%, bearing in mind that pores may act as stress raisers and the resultant stress concentration facilitates crack nucleation and growth.

SEM and EDX were employed to further characterize the microstructure with higher magnifications. Fig. 3-9 presents a closer view of the (WC-60Co)-10TiNi. Local composition of a dark domain marked by 2, which was between a cluster of TiNi phase and the Co matrix, was analyzed with EDX and results are given in Table 3-3. As shown, this dark domain contained different elements and should be a mixture of different phases. η value of this region was around 34%. Spots 1 and 4 were richer in Ti and showed higher η value and higher strength; they could

contain more TiNi alloy phase. Grey or dark grey areas marked by 3 and 5 were the Co matrix containing very low concentration of dissolved Ti.

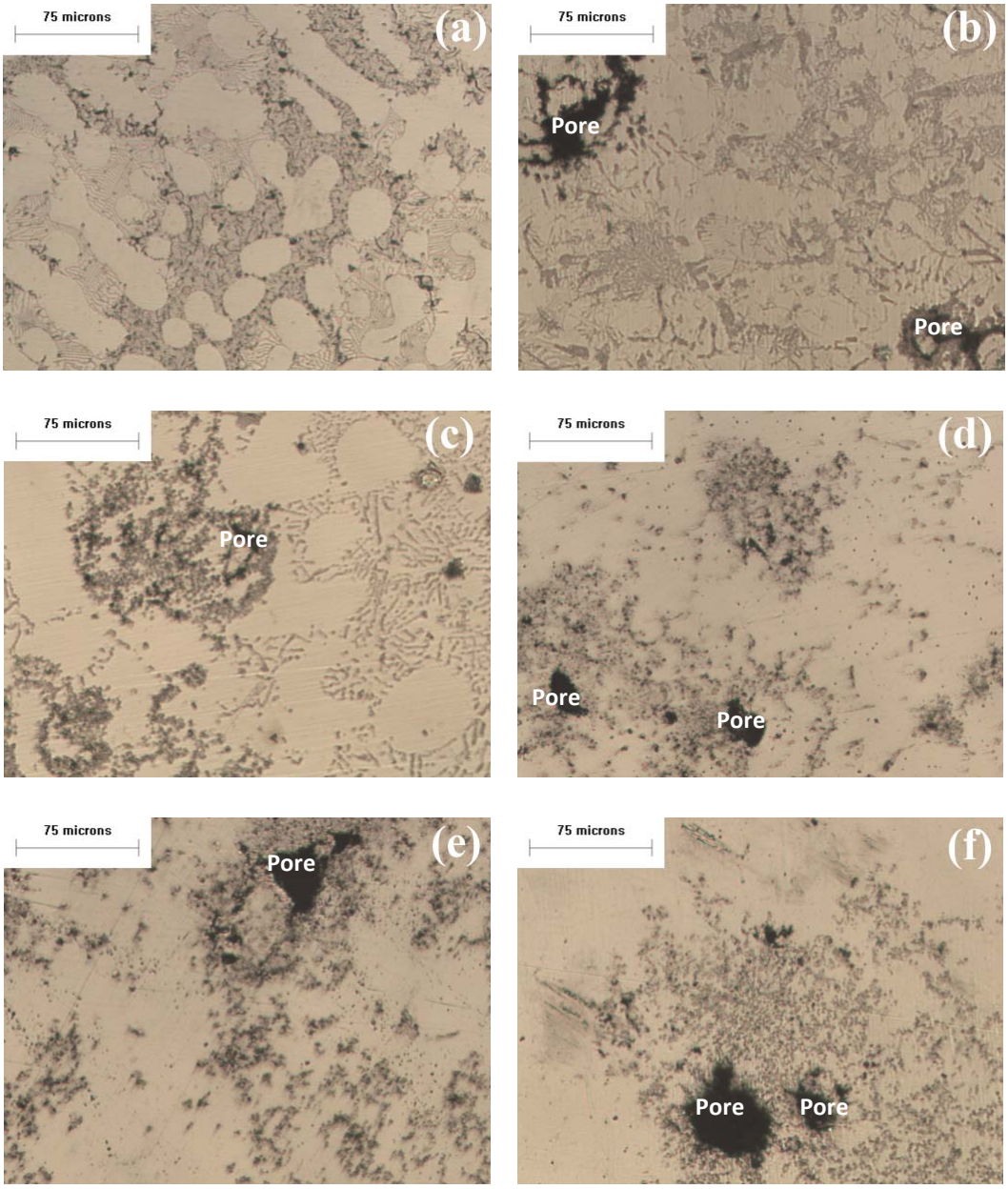

Fig. 3-8 Optical microscopic pictures of samples: (a) WC-60Co, (b) (WC-60Co)-5TiNi, (c) (WC-60Co)-10TiNi, (d) (WC-60Co)-15TiNi, (e) (WC-60Co)-20TiNi, and (f) (WC-60Co)-25TiNi. The dark areas are pores

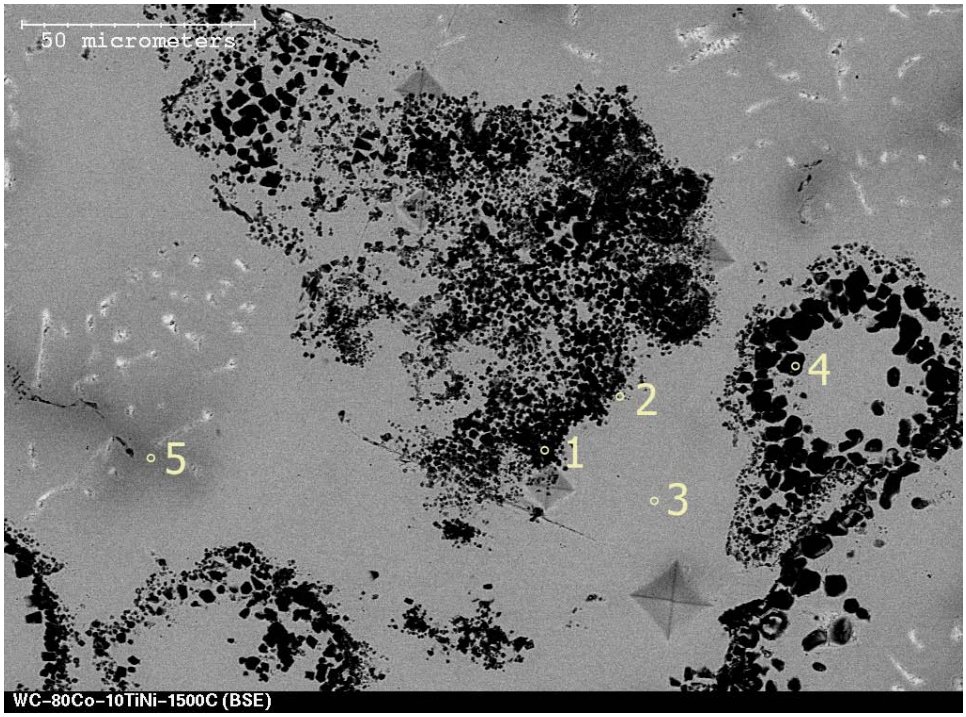

Fig. 3-9. A backscattered electron image of a (WC-60Co)-10TiNi sample

Table 3-3. Composition detected at spot 2 in Fig. 3-9

Elm	ZAF	Norm wt%	Prec.	Atomic %	Line
Ti	1.0233	4.4	0.21	6.18	K line
Co	0.9784	68.28	1.11	77.93	K line
Ni	0.9279	7.57	0.39	8.68	K line
W	1.6705	19.75	0.84	7.22	M line

The sample was also analyzed using XRD. The following phases, titanium carbides (in forms of TiC and Ti_8C_5), Co_6W_6C, titanium nickel (in forms of TiNi and $Ti_{1.33}Ni_{2.67}$), Co_3Ti, tungsten carbide (in form of WC_{1-x}) and titanium tungsten carbide (in form of $(W, Ti)C_{1-x}$), were detected in the XRD pattern of the sample

as illustrated in Fig. 3-10. According to the XRD pattern, decomposition of TiNi and WC more or less occurred, and the released elements reacted with Co to a certain degree. However, TiNi phase was retained in the composites, which should be within those dark domains.

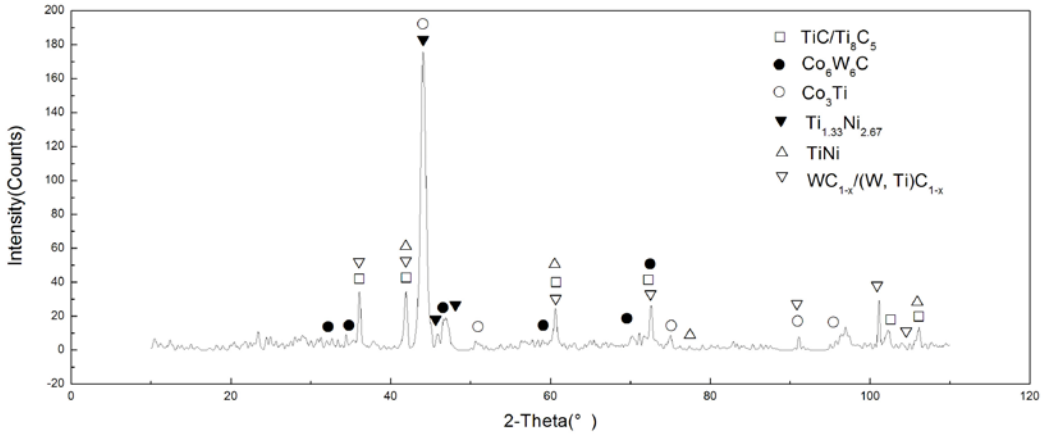

Fig. 3-10. A XRD pattern of (WC-60Co)-10TiNi sample

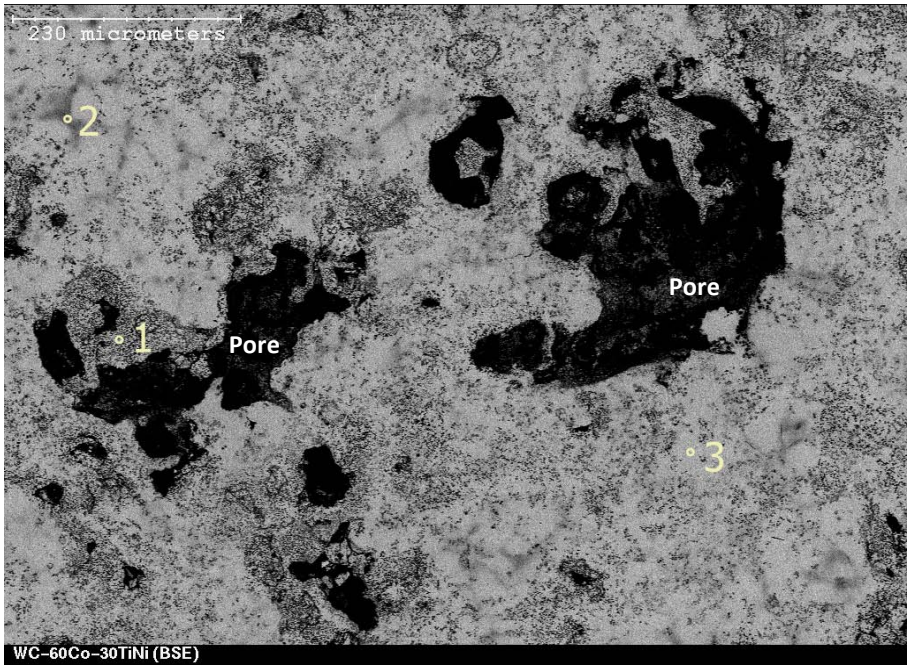

Fig. 3-11. A backscattered electron image of a (WC-60Co)-30TiNi sample

It has been shown earlier, adding TiNi alloy powder more than 10 wt% appeared to promote the formation of pores. In order to obtain more relevant information, a (WC-60Co)-30TiNi sample was examined using SEM and EDX with focus on the adjacent area of pores. As illustrated in Fig. 3-11, the grey areas marked by 2 and 3 contain a high Co content (about 67 at%) and a low Ti content (about 5 at%); while at spot 1, the Ti content is much higher (about 80 at%) along with about 16at%W and 2.4at%Co.

The above local compositional analysis may imply that the formation of pores could be triggered by the reactions among dissolved Ti, W and Co. How this happened and whether the formed compounds such as $(W,Ti)C_{1-x}$ and Co_3Ti as well as how the local phase decomposition affected the formation of pores needs further investigation.

3.4. Conclusions

Pseudoelastic TiNi powder was added to WC-60Co in an attempt to enhance the wear resistance of this composite. It was demonstrated that a small amount of TiNi powder (around 10wt%) resulted in markedly increased wear resistance. The microstructure characterization using SEM, EDX and XRD showed that pseudoelastic TiNi phase existed in the matrix although some decomposition occurred during sintering. The added pseudoelastic TiNi phase helped to reinforce the Co matrix and could also render it tougher. When the added TiNi exceeded 10

wt%, however, the positive effect of TiNi was weakened with the formation of pores, which could be responsible for the deterioration of wear resistance.

References

[1] W. A. Brainard, D. H. Buckley, Dynamic SEM wear studies of tungsten carbide cermets, Tribology Transactions 19 (1976) 309–318

[2] D. K. Shetty, I.G. Wright, P. N. Mincer, A. H. Clauer, Indentation fracture of WC-Co cermets, Journal of Materials Science 20 (1985) 1873–1882

[3] J. B. J. W. Hegeman, J. Th. M. De Hosson, G. de With, Grinding of WC-Co hardmetals, Wear 248 (2001) 187–196

[4] H. Klaasen, J. Kubarsepp, Abrasive wear performance of carbide composites, Wear 261 (2006) 520–526

[5] A. Koutsomichalis, N. Vaxevanidis, G. Petropoulos, E. Xatzaki, A. Mourlas, S. Antoniou, Tribological coatings for aerospace applications and the case of WC-Co plasma spray coatings, Tribology in industry 31 (2009) 37–42

[6] M. T. Laugier, Effect of hardness on erosion of WC-Co composites, J. of Mater.Sci. 21 (1986) 3548–3550

[7] J.L. Chermant, F. Osterstock, Fracture toughness and fracture of WC-Co composites, J. of Mater. Sci. 11 (1976) 1939–1951

[8] D. Han, J.J. Mecholsky Jr., Fracture behavior of metal particulate-reinforced WC-Co composites, Mater. Sci. and Eng. A 144 (1991) 293–302

[9] K. Jia, T.E. Fischer, B. Gallois, Microstructure, hardness and toughness of nanostructured and conventional WC-Co composites, NanoStructured Materials 10 (1998) 875–891

[10] W. Acchara, C. Zollfrankb, P. Greilb, Microstructure and mechanical properties of WC-Co reinforced with NbC, Materials Research 7 (2004) 445–450

[11] Z. Fang, G. Lockwood and A. Griffo, A dual composite of WC-Co, Metallurgical and Materials Transactions A 30 (1999) 3231–3238

[12] D.Y. Li, A New Type of Wear-resistant Material: Pseudo-elastic TiNi Alloy, Wear 221 (1998) 116

[13] D.Y. Li, Development of novel tribo composites with TiNi shape memory alloy matrix, Wear 255 (2003) 617

[14] Y. Shida and Y. Sugimoto, Water jet erosion behaviour of Ti-Ni binary alloys, Wear 146 (1991) 219–228

[15] R. Liu and D.Y. Li, Experimental Studies on Tribological Properties of Pseudoelastic TiNi Alloy with Comparison to Stainless Steel 304, Metall. Mater. Trans. A 31 (2000) 2773

[16] T. Zhang and D.Y. Li, Variation in erosion resistance of pseudoelastic TiNi alloy with respect to temperature, Mater. Sci. & Eng. A 329 (2002)

563.

[17] V.A. Chernenko, High pressure effects on the martensitic transformations, J. de Phys. IV, Colloque C2 5 (1995) C2–77.

[18] L. Tan, W.C. Crone, Surface characterization of NiTi modified by plasma source ion implantation. Acta Mater. 50 (2002) 4449–4460

[19] ASTM Standard G 99-05, Standard Test Method for Wear Testing with a Pin-on-Disk Apparatus, Annual Book of ASTM Standards, vol. 03.02, 2005

[20] Shoji Miyake, Novel materials processing by advanced electromagnetic energy sources, Elsevier Science, 2005

[21] R. Liu, D.Y. Li, Y.S. Xie, R. Liewellyn, and H.M. Hawthorne, Indentation Behaviour of Pseudoelastic TiNi Alloy, Scripta Mater. 41 (1999) 691–699

Chapter 4

Wear performances of WC-TiNi and TiC-TiNi in comparison with that of WC-Co

Chapter 4 - Wear performances of WC-TiNi and TiC-TiNi in comparison with that of WC-Co

4.1. Introduction

The study reported in chapter 3 demonstrates that the wear performance of WC-Co composites can be improved by adding pseudo-elastic TiNi alloy powder to increase the wear resistance of the Co matrix while keeping the matrix flexible. However, when the amount of added TiNi powder exceeded the mass amount of 10%, the beneficial effect of TiNi was diminished. Since for commercially used WC-Co composites the mass percentage of Co usually ranges from 3% to 30% [1-2], another batch of samples with Co content of 30wt% were prepared in the same routine as described in chapter 3 to approach the real scenario. From the test results shown in Fig. 4-1, it can be drawn again that a small amount of TiNi alloy can be advantageous to the wear resistance of WC-Co composite. However, it was also observed that in this case, the benefit of TiNi was negligible due to elevated formation of pores.

Since TiNi alloy possesses high ductility, good wear resistance due to its pseudo-elasticity [3-15], and great flexibility which makes it more effective to absorb impact energy [15-17], an alternative approach was tried by replacing the Co matrix of WC-Co with TiNi completely in this study. However, the compatibility between WC and TiNi is a possible issue but little relevant information is available. Thus, it is worth investigating WC-TiNi composites as a potential wear-

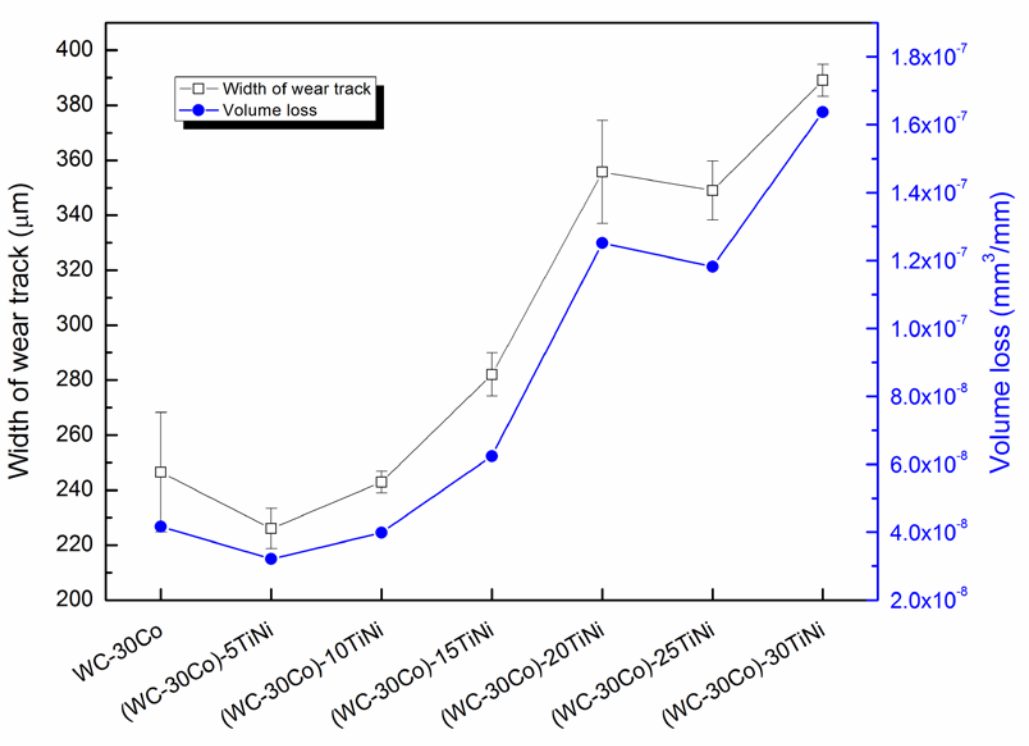

Fig. 4-1. The width of wear track and calculated volume loss of different samples worn under a load of 10N at a speed of 0.5cm/s for 10000 laps

resistant material. Besides, for the purpose of avoiding possible problems with weak interfacial bonding and comparing with WC-TiNi composite, TiC was used as the reinforcing phase which could be compatible with TiNi to fabricate TiC-TiNi composite. Previous studies have shown that TiNi alloy reinforced by TiC particles exhibits improved wear resistance [18-21]. Therefore, there is no main concern about the bonding at TiC-TiNi interface. In this work, WC-TiNi and TiC-TiNi composites were fabricated and their wear resistances were evaluated and compared to that of WC-Co. The objective of this study is to determine whether it is possible to replace Co with pseudo-elastic TiNi alloy and whether WC-TiNi or

TiC-TiNi composite could be potential substitutes for the well-known WC-Co composite. Efforts were also made to clarify relevant mechanisms.

4.2. Experimental Details

WC powder (99.5%) and TiC powder (99%) were purchased from Strem Chemicals; Co powder (99.8%, metal basis, -100+325 mesh, spherical) was provided by Alfa Aesar; pseudoelastic TiNi alloy powder was provided by SAES smart materials (-80+100 mesh) with the composition in the range from Ti-55wt%Ni to Ti-56.5wt%Ni.

The first group of specimens with the composition of WC-60vol%Co, WC-60vol%TiNi and TiC-60vol%TiNi were prepared and sintered to compare their wear resistance.

Powders were weighed according to Table 4-1, mixed using the dry ball milling method, cold pressed to green specimens and then sintered using a hot isostatic pressing (HIP) furnace (HP630, AIP, USA) in argon atmosphere. The sintering process proceeded following the scheme shown in Fig. 4-2. The sintering temperature was set the same as in chapter 3 for the following reasons: 1) it is advisable that the sintering temperature be slightly higher than the melting temperature of TiNi alloy which is 1310^{o}C, so that there would be an appropriate amount of liquid phase during sintering to reduce the pores of the pellet; 2) the temperature was applied by H.Z. Ye [21], and it was proved that 1500^{o}C is a

proper temperature to retain the shape of the ceramic-reinforced TiNi alloy matrix composites without generating too much liquid phase.

Specimens were tested on a pin-on-disk tribometer for 10000 laps at a linear speed of 0.5cm/s and under a load of 10N to form a wear track, as a representative wear track is shown in Fig. 4-3. The profiles of the wear tracks (Fig. 4-4) were determined with a Zeiss Axio CSM 700 confocal microscope and the volume losses were integrated accordingly in order to evaluate their sliding wear behavior.

Table 4-1. Fractions of powders for different specimens

	Volume percentage			
Sample No.	Co	TiNi	WC	TiC
1	60%	0%	40%	0%
2	0%	60%	40%	0%
3	0%	60%	0%	40%

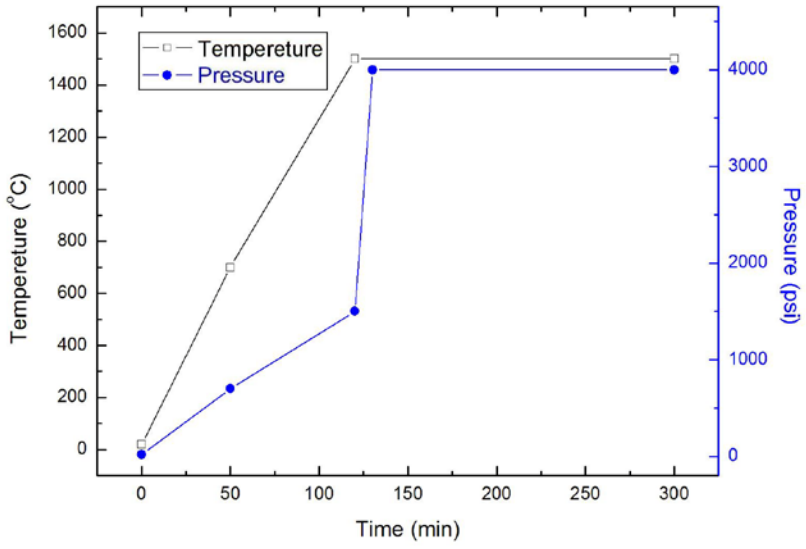

Fig. 4-2. Temperature and pressure versus time for sintering

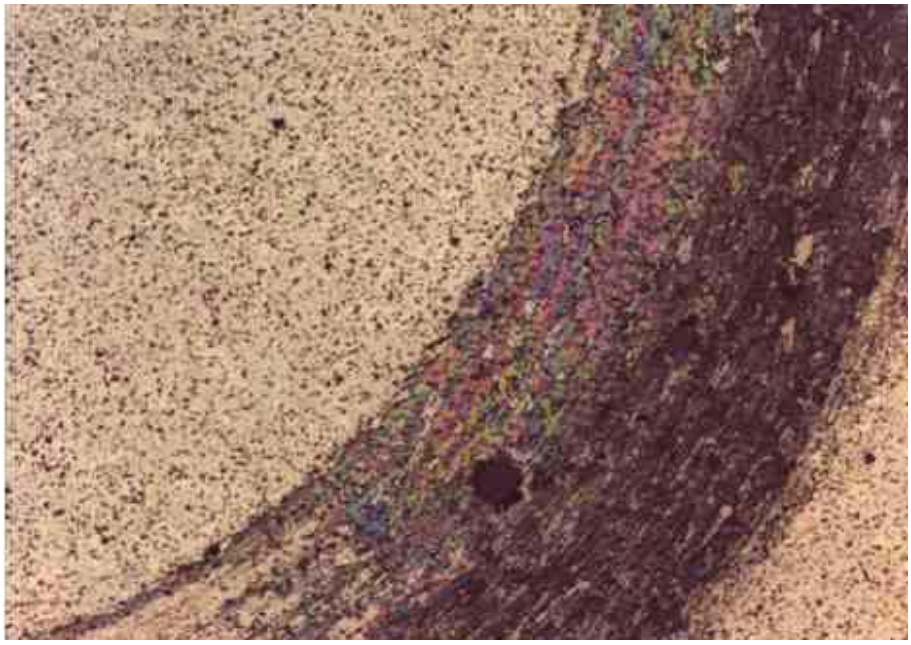

Fig. 4-3. A representative of wear track on specimen of WC-60vol%TiNi

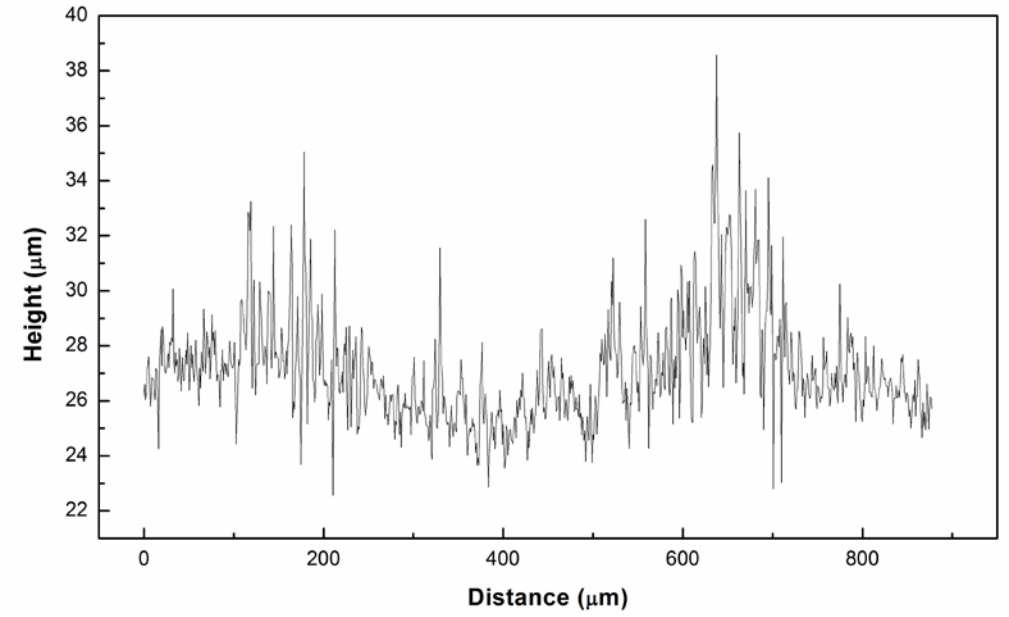

Fig. 4-4. A representative wear track profile on specimen of TiC-20vol%TiNi

In many commercial applications, tribo-composites such as WC-Co usually have the fractions of the metal matrix lower than 60%vol and weight percentage is commonly used, such as WC-30wt%Co. Since it is more advisable to compare the wear resistance of different specimens with volume fraction, WC-30wt%Co composite was converted to WC-43vol%Co, besides, specimens with composition of WC-43vol%TiNi and TiC-43vol%TiNi were prepared accordingly.

4.3. Results and discussion

4.3.1. Wear behavior of WC-60vol%Co, WC-60vol%TiNi and TiC-60vol%TiNi

After tested with the pin-on-disc wear tester, profile of wear tracks on WC-60vol%Co, WC-60vol%TiNi and TiC-60vol%TiNi were obtained and the volume losses of the three samples were then calculated. Results of the calculations are presented in Fig. 4-5.

As shown, both TiC-60vol%TiNi and WC-60vol%TiNi demonstrated higher wear resistance than WC-60vol%Co, and TiC-60vol%TiNi exhibited the highest wear resistance. When the pseudo-elastic TiNi alloy is used as the metal matrix, it provides higher capability to accommodate large-scale deformation for high-stress abrasion and to absorb impact energy from impact wear with less damage, compared to conventional metal matrix. Since TiNi alloy itself has high wear resistance [15], such composites are resistant to wear under various wearing conditions. So the superiority of the TiNi-matrix composites can be expected. Between TiC-60vol%TiNi and WC-60vol%TiNi, the former contains harder

ceramic phase and particularly has better interfacial bonding between the reinforcing phase and the matrix, thus showing a higher wear resistance.

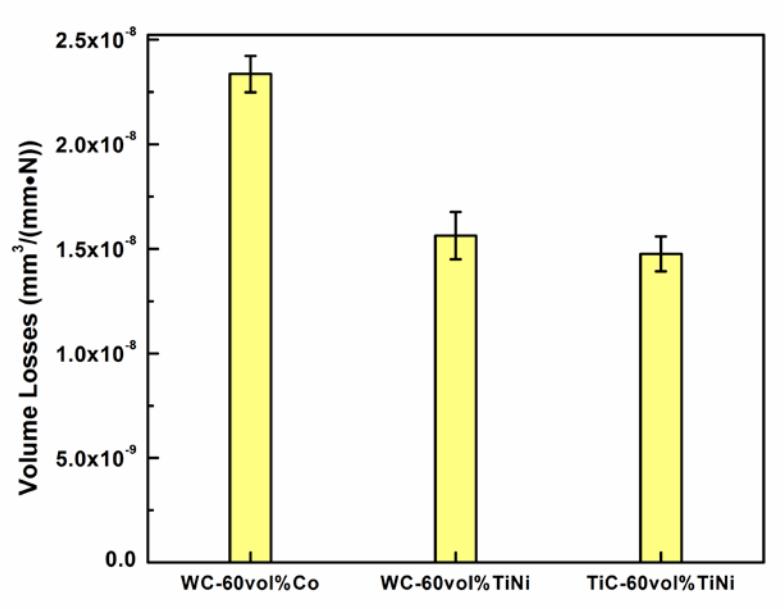

Fig. 4-5. Volume losses of WC-60vol%Co, WC-60vol%TiNi and TiC-60vol%TiNi

As mentioned earlier, the volume fraction of the metallic matrix is usually lower, e.g., WC-30wt%Co (or WC-43vol%Co). So, specimens of WC-43vol%Co, WC-43vol%TiNi and TiC-43vol%TiNi were also made and tested to evaluate their wear resistances under the same testing condition. Results of the wear tests are presented in Fig. 4-6.

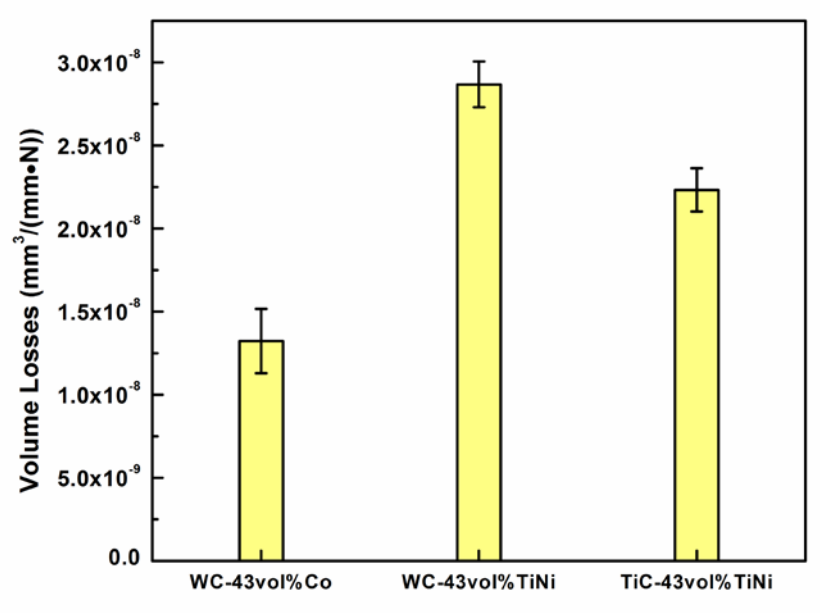

Fig. 4-6. Volume losses of WC-43vol%Co, WC-43vol%TiNi and TiC-43vol%TiNi

When the volume fraction of metal matrix in the composites was decreased, the sequence of wear resistance altered remarkably. The specimen of WC-43vol%Co rendered the best wear resistance, followed by the specimen of TiC-43vol%TiNi, while the specimen of WC-43vol%TiNi showed the widest wear track and the largest volume loss. A possible explanation is that the hard carbides particles tended to be pulled off more easily when the fraction of metal matrix became lower; for the specimen of WC-43vol%TiNi, the interfacial bonding or the compatibility between carbide and metal matrix phase was not as strong or high as those of other two specimens and detrimental reactions could have occurred, leading to the formation of pores in the sintered pellet (this has been shown in later part of this chapter) and it turned to be the poorest wear-resistant specimen among the three.

The same trend was observed when the volume fraction of the metal matrix was further decreased to 20 volumetric percentages, as shown in Fig. 4-7. By checking the microstructure of the composites, higher porosity was found in both specimens of WC-20vol%TiNi and TiC-20vol%TiN (as demonstrated and discussed in section of 4.3.2 - Microstructures and compositions of various samples) when compared to specimens of WC-43vol%Co and TiC-43vol%TiNi, respectively.

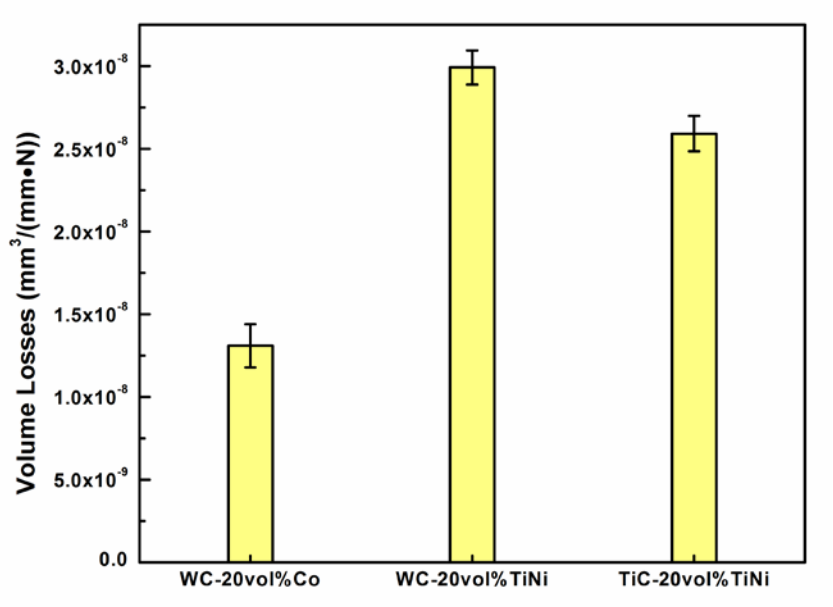

Fig. 4-7. Volume losses of WC-20vol%Co, WC-20vol%TiNi and TiC-20vol%TiNi

For better comparison, the wear losses of all tested samples are presented in Fig. 4-8. One may see that the wear resistance of WC-Co composites increased when the volume fraction of Co was decreased; whereas the wear resistance of WC-TiNi and TiC-TiNi composites decreased when the volume fractions of TiNi were reduced.

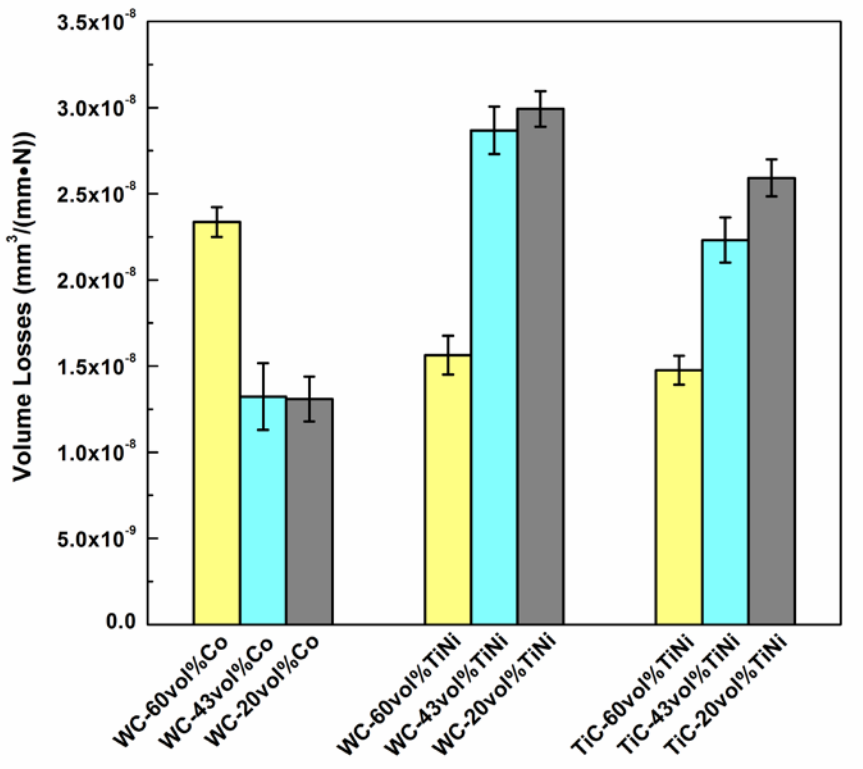

Fig. 4-8. Volume losses of WC-20, 43, 60vol%Co, WC-20, 43, 60vol%TiNi and TiC-20, 43, 60vol%TiNi

In order to understand the trend of changes in the wear resistance of the samples with respect to the volume fraction of the metal matrix, macro-hardness of the samples was measured using a Mitutoyo AVK-C1 hardness tester. Results of the harness measurement are presented in Figure 4-9. As expected, the macro-hardness of WC-Co composite increased with the decrease in the Co volume fraction, which explains the improvement in the wear resistance of WC-Co when the volume fraction of the reinforcing phase WC is higher since the wear resistance is proportional to hardness. The hardness of TiC-TiNi composites showed a similar trend of variation as the volume fraction of TiNi was decreased.

However, this rule did not apply to the WC-TiNi composite due to the fact that pores formed when the fraction of TiNi was lowered (see the section of 4.3.2 - Microstructures and compositions of various samples). It was observed that WC-43vol%TiNi and WC-20vol%TiNi had high levels of porosity (will be shown later), which considerably reduced the load bearing capability and thus led to lower hardness. The wear resistance of these porous samples was correspondingly decreased.

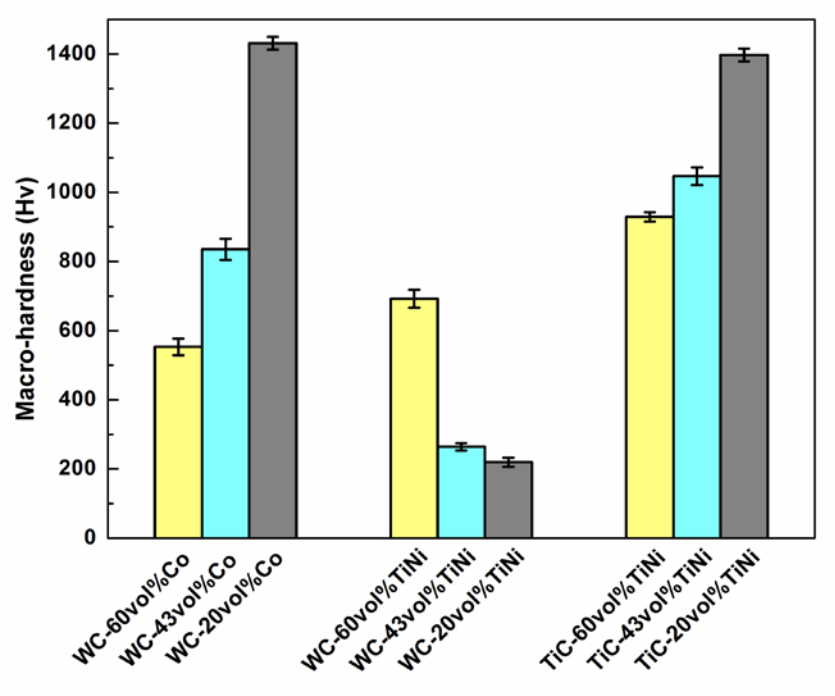

Fig. 4-9. Macro-hardness of WC-20, 43, 60vol%Co, WC-20, 43, 60vol%TiNi and TiC-20, 43, 60vol%TiNi

When the samples were comparatively free of pores or had more pseudo-elastic phase, such as TiC-60vol%TiNi, WC-60vol%TiNi and WC-60vol%Co, the wear resistance largely depended on the hardness or content of the pseudo-elastic phase.

From Figure 4-9, it can be seen that the hardness of TiC-60vol%TiNi is higher than that of WC-60vol%TiNi which is in accordance with the fact that TiC particles are harder than WC particles and possibly have stronger interfacial bonding with the TiNi matrix.

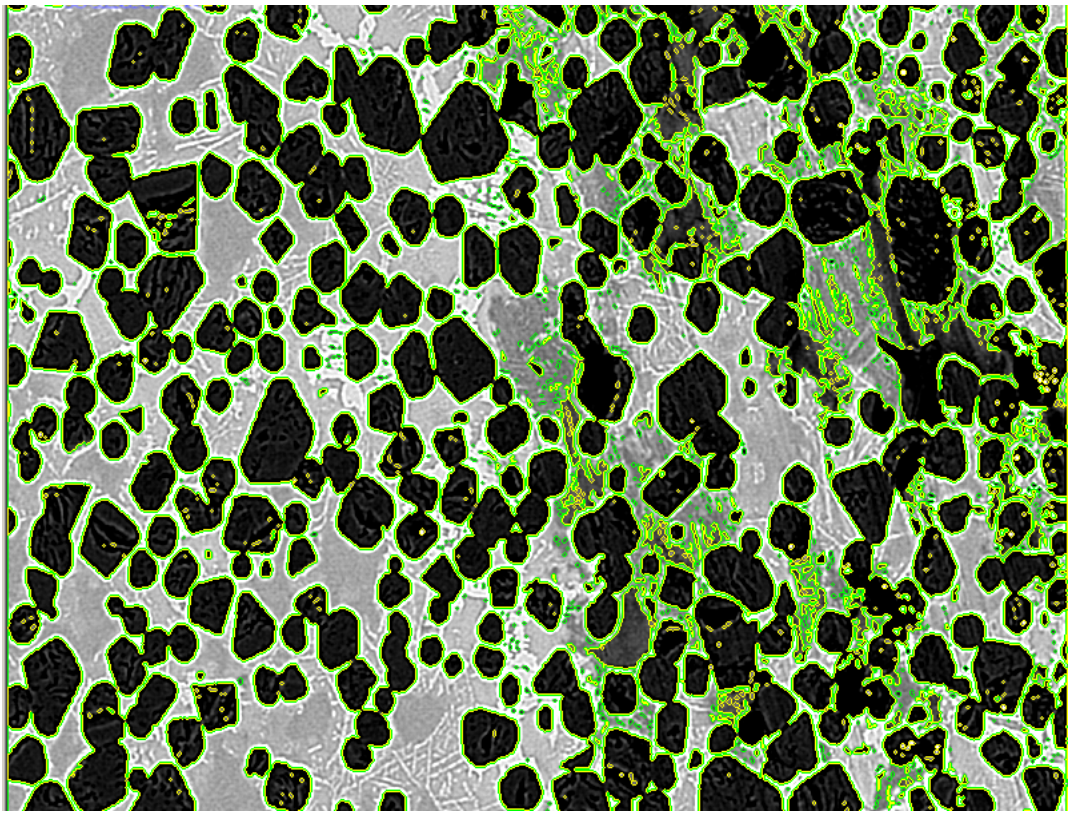

Fig. 4-10. A representative picture of counting different phases (TiC-60vol%TiNi)

In order to better understand the observed phenomena, the actual fractions of the reinforcing phase and the matrix in the samples were determined based on image analysis. Fig.4-10 presents an image of TiC particle distribution in TiC-60vol%TiNi, taken with SEM. In order to determine the fraction of TiC, the areas of different phases were processed with Image Pro based on the gray scales. In the

picture, dark areas are hard particles such as TiC, and the rest gray areas are taken as the matrix phase. Pores can also be identified (see the section of 4.3.2 - Microstructures and compositions of various samples). All samples were examined in the same way.

Table 4-2. Areal percentage of different phases in WC-60vol%Co, WC-60vol%TiNi and TiC-60vol%TiNi

	Porosity	Hard phase	Matrix
WC-60vol%Co	N/A	44.62	55.38
WC-60vol%TiNi	5.9	52.96	41.14
TiC-60vol%TiNi	N/A	56.84	43.16

As shown in Table 4-2, the actual percentages of hard phases deviated from the nominal ones either due to the losses of powders in mixing procedure or the reaction in sintering process. Despite the deviation, there was consensus in the increase of the areal percentage of hard phase and that of macro-hardness of these samples.

Micro-indentation was carried out on WC-60vol%TiNi and TiC-60vol%TiNi samples to confirm the existence of pseudo-elasticity (PE) of the matrix using η value (ratio of elastic deformation energy (W_e) to the total deformation energy (W_{tot})) as a characteristic parameter. Table 4-3 shows that η values of the two

samples are higher than 40%, indicating that the TiNi matrix is pseudo-elastic but some loss of pseudo-elasticity was observed in the WC-60vol%TiNi sample.

Table 4-3. Results of the micro-indentation on WC-60vol%TiNi and TiC-60vol%TiNi under a maximum load of 500 mN

	W_e/W_{tot} (η, %)	Hv	h_{max} (μm)
WC-60vol%TiNi	42.45	826.75	1.25
TiC-60vol%TiNi	46.14	1211.65	1.51

4.3.2. Microstructures and compositions of various samples

Since WC-Co is a commercial tribological composite, it has good compatibility between WC and Co and there are seldom pores in the composite after sintering, thus the composite is generally compact despite the volume fraction of the metal matrix. When the volume fraction of Co matrix decreased, the specimen became harder due to increased volume fraction of the ceramic phase and hence demonstrated higher wear resistance.

Wear tracks of specimens of WC-60vol%Co and WC-43vol%Co were observed with SEM and images of the wear tracks are illustrated in Fig. 4-11 and Fig. 4-12. One may see that the worn surface of the WC-Co samples was relatively homogeneous without cracking or obvious pull-off of WC particles. These may

imply that the interfacial bonding between WC and Co is strong and toughness of the composites is reasonably good.

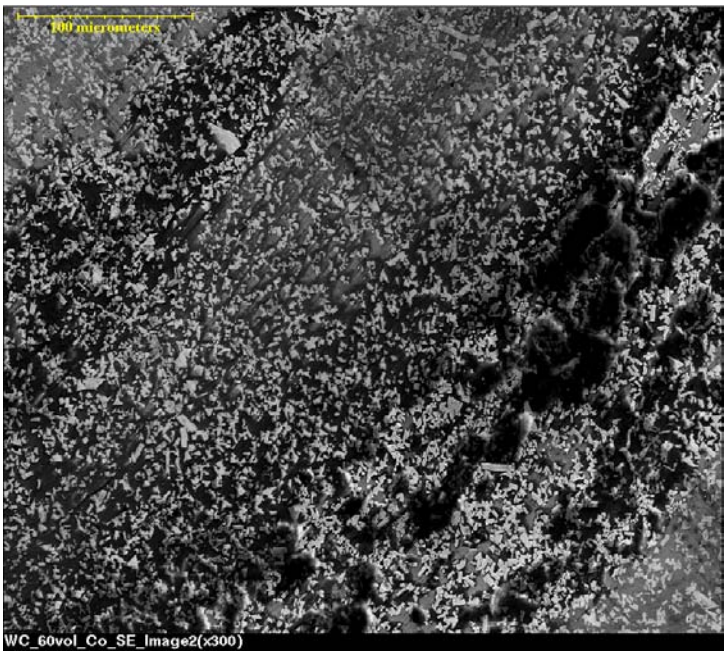

Fig. 4-11. A SEM image of wear track on WC-60vol%Co (X300)

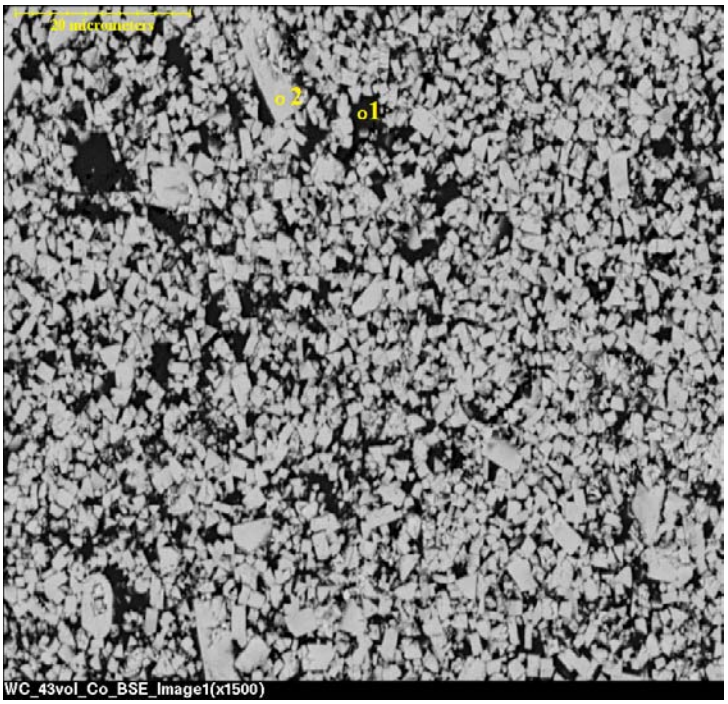

Fig. 4-12. A SEM image of wear track on WC-43vol%Co (X1500)

Compositions of the two main phases in these samples were determined using EDS and results are given in Table 4-4. As shown, the examined spots 1 (Co) and 2 (WC) keep high concentrations of Co and W respectively, which may be an indication that WC and Co only interact around the interface and there is not much interference to structural integrity of individual phases and thus their properties and roles were well retained in the composite.

Table 4-4. Composition detected in WC-43vol%Co sample in Fig. 4-12

	Atomic %	
Element	Spot 1	Spot 2
Co	91.13	5.06
W	8.87	94.93

For WC-60vol%TiNi, the wear resistance was improved with the pseudo-elastic TiNi matrix. However, the wear resistance decreased when the volume fraction of TiNi matrix was reduced, because a small amount of TiNi does not provide sufficient pseudo-elasticity to compensate for the disadvantage of weak interfacial bonding between WC and TiNi.

Phase analysis was carried out for TiC-20vol%TiNi, WC-20vol%TiNi, TiC-60vol%TiNi and WC-60vol%TiNi using X-ray diffraction technique. XRD patterns of the sample are illustrated in from Fig. 4-13 to Fig. 4-16. It was demonstrated that the TiNi alloy phase was still present in the composites with

60vol%TiNi after sintering (though decomposition existed) but no TiNi alloy phase remained in the composites when its volumetric fraction was 20%, indicating that the TiNi alloy phase had decomposed during sintering or reacted with the reinforcing phase, thus losing the pseudo-elasticity. This negatively affected the wear resistance of the composites.

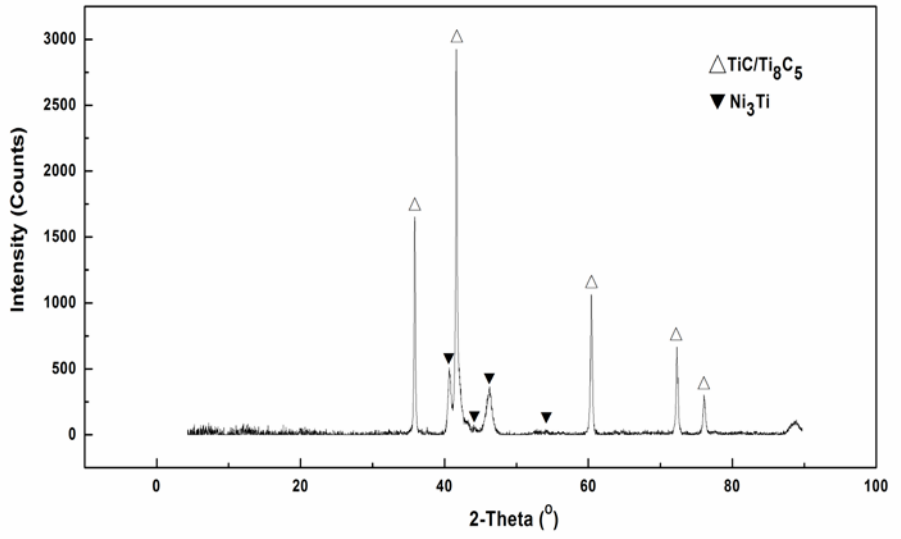

Fig. 4-13. A XRD pattern of TiC-20vol%TiNi

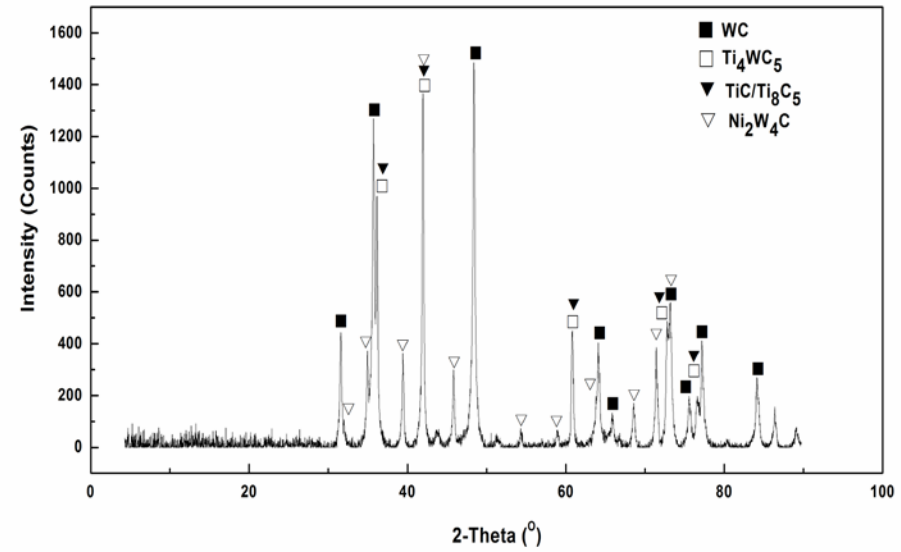

Fig. 4-14. A XRD pattern of WC-20vol%TiNi

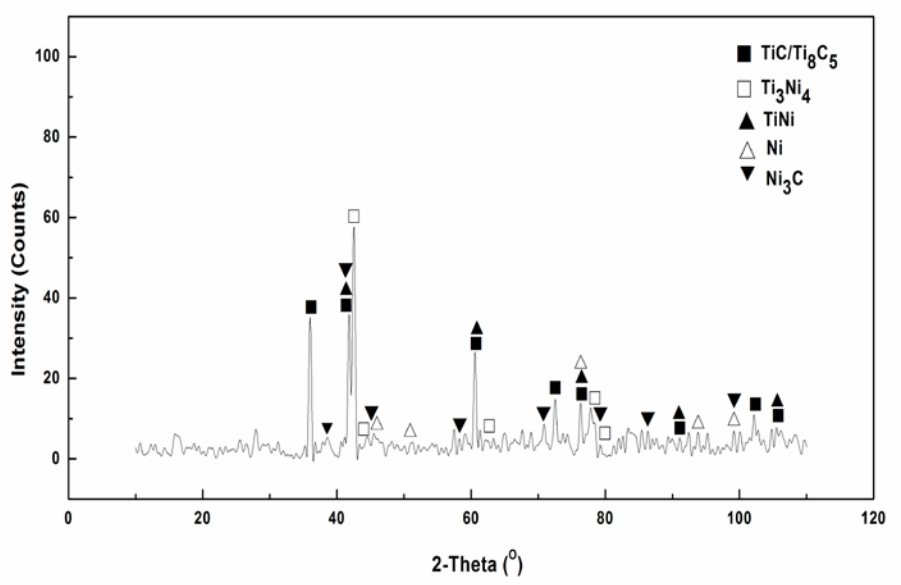

Fig. 4-15. A XRD pattern of TiC-60vol%TiNi

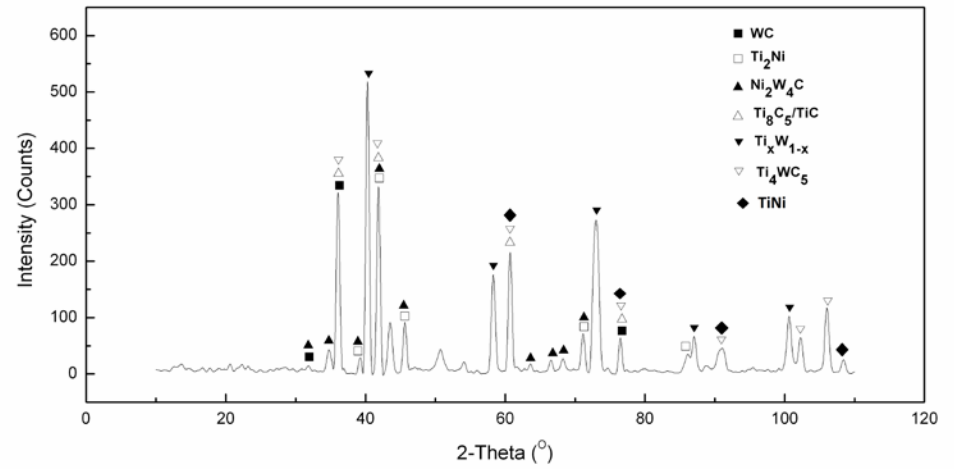

Fig. 4-16. A XRD pattern of WC-60vol%TiNi

In order to understand the poor performance of WC-TiNi with low volume fraction of TiNi, micro-structures of WC-43vol%TiNi and WC-20vol%TiNi samples were examined with SEM. Fig. 4-17 shows the micro-structure of a WC-43vol%Co specimen. As shown, pores formed in the specimen and the

microstructure was inhomogeneous or disordered. Local composition was analyzed using EDX and compositions of different domains are listed in Table 4-5.

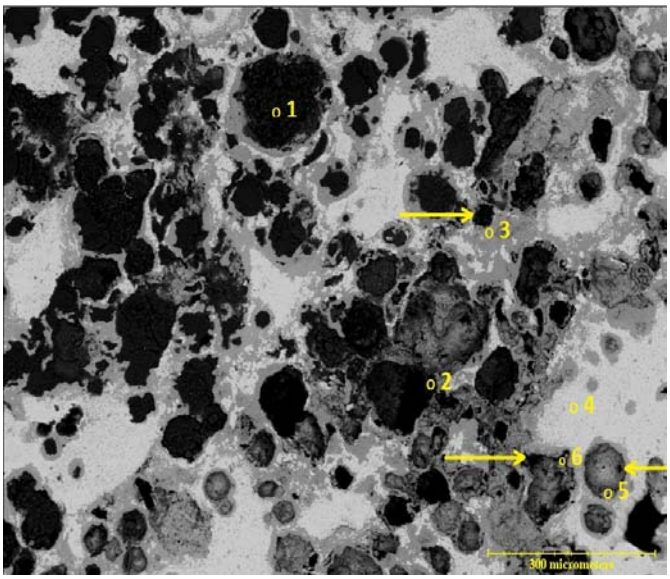

Fig. 4-17 A back scattered electron image of WC-43vol%TiNi after wear test (X100)

Table 4-5. Compositions of different spots in the WC-43vol%TiNi sample shown in Fig. 4-17

	Atomic %					
Element	1	2	3	4	5	6
Ti	3.34	6.59	66.59	---	61.73	55.54
Ni	2.14	4.85	3.15	36.96	3.28	7.95
W	81.06	73.57	30.25	63.04	34.99	36.50
Si	5.47	8.83	---	---	---	---

The spots 1 and 2 in the dark areas (oppositely bright areas in secondary electron image) are rich in composition of W, and located within hard phase of WC. The

small amount of Si in these areas came from the Si_3N_4 pinning ball, because this observation was done after the wear test. Spots 3, 5 and 6, which are close to the pores (shown by arrows), are all rich in composition of Ti and W while the light area is composed of Ni, W and C, possibly Ni_2W_4C which is revealed in XRD test in Fig. 4-14 and Fig. 4-16.

As to porosity, the specimens of WC-20vol%TiNi and TiC-20vol%TiNi were analyzed to further look into this issue. Since the observations were conducted after the wear tests, there might be traces of Si element present in EDX analysis. The areas with pores in WC-20vol%TiNi and TiC-20vol%TiNi, separately shown in Fig. 4-18 and Fig. 4-19, were analyzed using EDX technique. Results of the compositional analysis are given in Table 4-6 and Table 4-7, respectively.

An area which is away from the wear track on the sample of WC-20vol%TiNi was observed. As shown in Fig. 4-18, there are pores in the dark domains (indicated with arrow) According to H. Tanaka [22] and X.H. Wang [23], the equations for standard Gibbs free energy of formation of WC and TiC are

$$\Delta G^o = -38000 - 8.4T \text{ J mol}^{-1} \quad (4\text{-}1)$$

and

$$\Delta G^o = -186731+13.2T \text{ J mol}^{-1} \quad (4\text{-}2)$$

respectively. Obviously, at the temperature of 1500^{o}C, i.e. 1773.15K, ΔG^o (-181056.92 J mol^{-1}) of TiC is more negative than ΔG^o (-52894.46 J mol^{-1}) of WC, so Ti tends to react with WC to form TiC rather than remaining in TiNi alloy. Although the formed TiC has a lower density than WC, it dissolves 73% by wt. of WC at the temperature of 1400^{o}C [24], which might be the main reason why

cracks or pore were generated around Ti and W rich regions as spots 1, 2 and 5 indicated (see Table 4-6). These made the composite brittle with the formation of high-density cracks during wear.

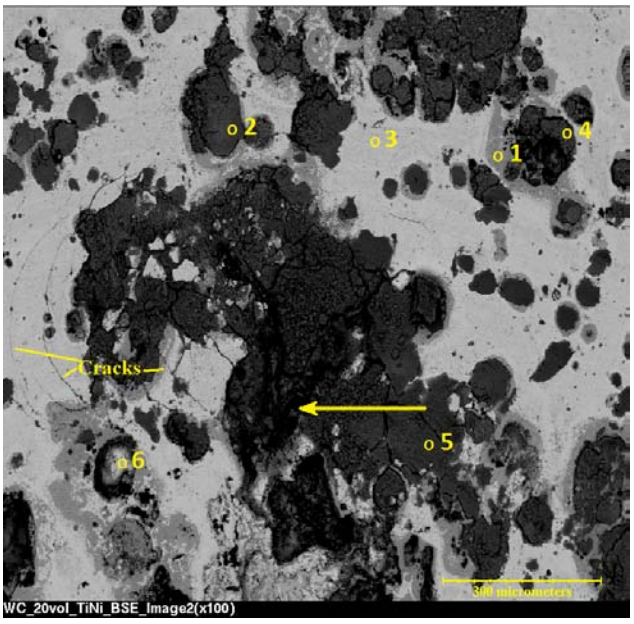

Fig. 4-18. Back scattered electron image of WC-20vol%TiNi (X100)

Table 4-6. Composition detected in WC-20vol%TiNi sample in Fig. 4-18

	Atomic %					
Element	1	2	3	4	5	6
Ti	60.08	16.17	4.94	8.19	16.91	3.31
Ni	---	21.21	4.29	17.65	21.07	33.78
W	39.93	62.57	90.77	74.14	62.03	62.91

Fig. 4-19 illustrates the microstructure of a TiC-20vol%TiNi composite after the wear test, and the image includes some part of the wear track as there is Si detected on spot 3. In the composite, reactions also occurred between TiC and TiNi. As shown, for areas of TiC/Ti_8C_5 as marked with arrows, pores tend to form

around them. Apart from the porosity, the rest of the material is only composed of two phases, Ni_3Ti and TiC/Ti_8C_5, and Ni_3Ti possesses a higher density when compared to titanium carbides or titanium nickel [25]. Combining with the result in Fig. 4-15, there was no TiNi alloy left in the composite. The formation of the pores could be ascribed to the shrinkage around Ni_3Ti during sintering and the brittleness of the hard phases.

SEM and EDX tests were also applied to determine if there were remaining TiNi alloy phase (see Table 4-7). It appears that near equi-atomic TiNi alloy barely remained due to decomposition and interaction with TiC.

Table 4-7. Composition detected in TiC-20vol%TiNi sample in Fig. 4-19

	Atomic %		
Element	1	2	3
Ti	100	69.24	67.12
Ni	0	30.75	6.10
Si	---	---	26.78

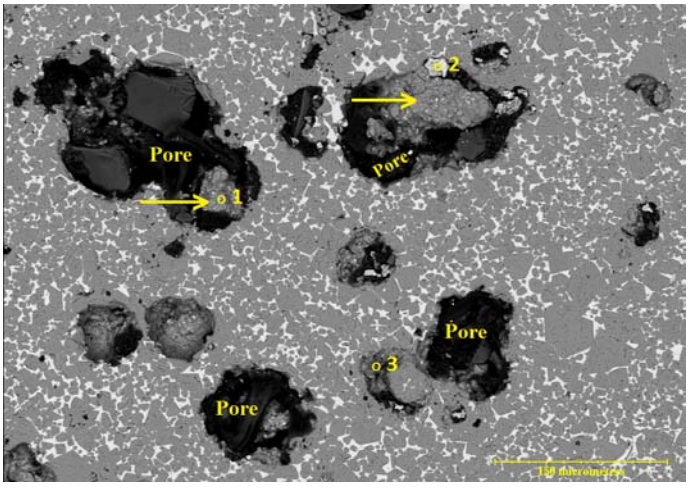

Fig. 4-19. Back scattered electron image of TiC-20vol%TiNi (X200)

The above results show that the TiNi alloy phase had decomposed in the composites with low volume fractions of TiNi, leading to deteriorated wear resistance. Since composites with high volume fraction of TiNi demonstrated improved wear resistance, microstructures of the WC-60vol%TiNi and TiC-60vol%TiNi composites were examined with SEM and EDX.

Figure 4-20 illustrates a back scattered electron image of TiC-60vol%TiNi and local compositions were measured and given in Table 4-8. As shown, no pores existed in the composite. The composition of spot 3 is Ti-53.72at%Ni, which is close to that of pseudoelastic TiNi alloy, implying the grey areas may mainly consist of TiNi alloy, and further explaining why this composite performed well during wear testing.

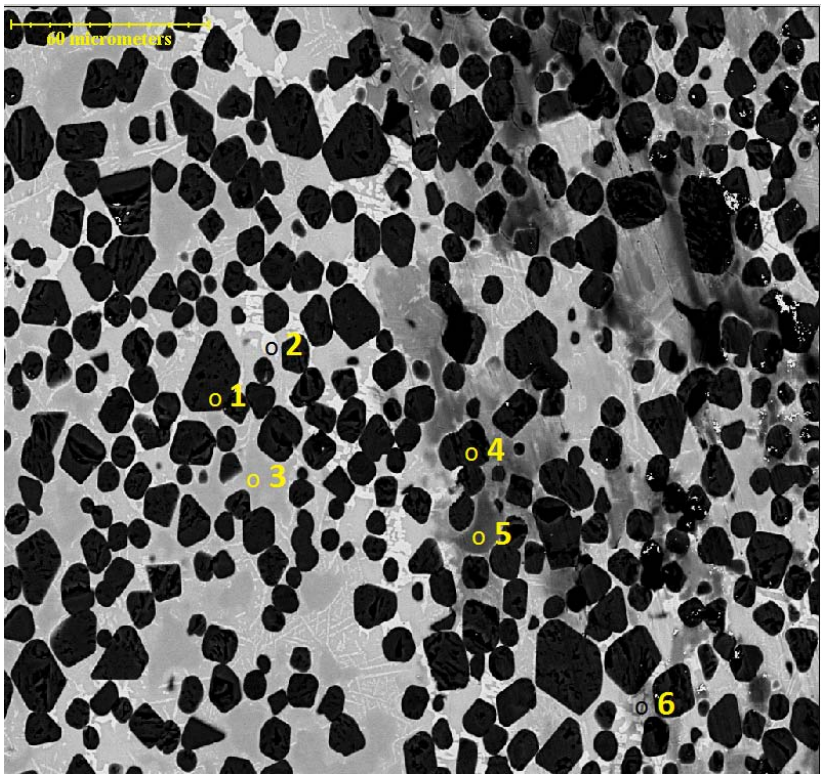

Fig. 4-20. Back scattered electron image of TiC-60vol%TiNi (X500)

Table 4-8. Composition detected in TiC-60vol%TiNi sample in Fig. 4-20

	Atomic %	
Element	2	3
Ti	25.81	46.28
Ni	74.19	53.72

For the sample of WC-60vol%TiNi, its microstructure is demonstrated with a back scattered electron image as Fig. 4-21. Different from that of WC-TiNi composites with lower volume fraction of TiNi, no pores were observed in this composite. In addition, spot 2 has the composition of Ti-54.85at%Ni, which is close to that of the pseudoelastic TiNi alloy again (see Table 4-9). These may explain why WC-60vol%TiNi exhibited higher wear resistance than WC-60vol%Co as shown in Fig.4-8.

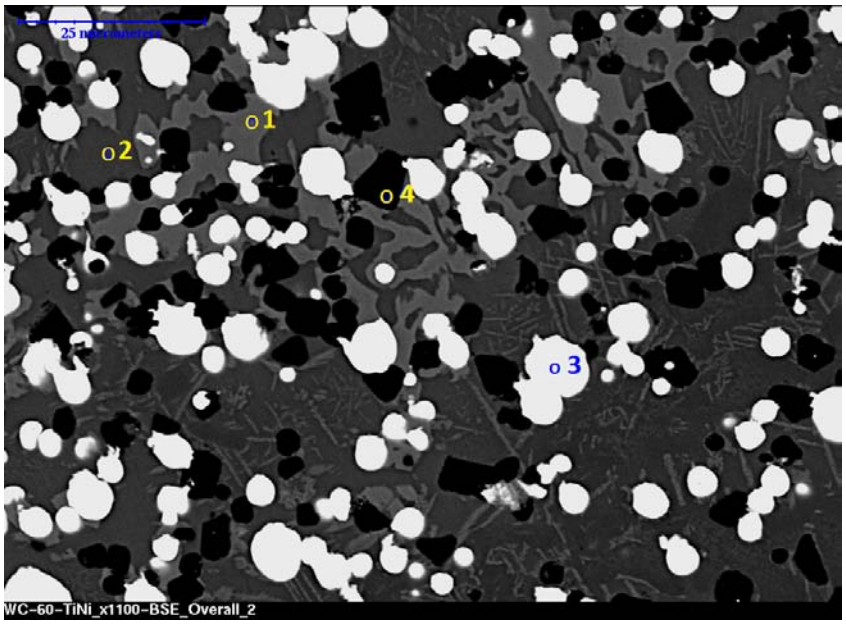

Fig. 4-21. A back scattered electron image of WC-60vol%TiNi (X1100)

Table 4-9. Compositions of two spots in the matrix of WC-60vol%TiNi sample shown in Fig. 4-21

Atomic %		
Element	1	2
Ti	24.89	45.15
Ni	74.69	54.85
W	0.37	---

However, it is unclear why pores formed in WC-TiNi composites with low volume fractions of TiNi but no obvious formation of pores in WC-60vol%TiNi. The formation of pores could be affected by many factors, such as the chemical compatibility between WC and TiNi, the lattice mismatch stress at WC-TiNi interface, the spacing between WC particles which influences the overall lattice mismatch stress, thermal stress due to the difference in thermal expansion coefficient between WC and TiNi and atomic diffusion, etc. Further studies are needed in order to understand why pores only formed in WC-TiNi with low volume fraction of TiNi matrix.

4.4. Conclusions

The near equi-atomic TiNi alloy with pseudo-elasticity and high resistance to wear was used as the matrix to form composites with carbides. Microstructure and wear resistance of WC-TiNi and TiC-TiNi composites with 60vol%TiNi,

43vol%TiNi and 20vol%TiNi were respectively characterized and evaluated. The following conclusions are drawn:

1) The wear resistance of WC-Co composite is inferior to those of WC-TiNi and TiC-TiNi composites when the volume fraction of the metal matrix is relatively high, such as 60vol%. However, the situation is reversed when the volume fraction of the metal matrix is lower.

2) The wear resistance of WC-Co composites increased when the volume fraction of Co was reduced; whereas the wear resistance of WC-TiNi and TiC-TiNi composites decreased when the fractions of TiNi were reduced. This could be ascribed to the fact that TiNi alloy may not be well retained due to its lower compatibility with the reinforcing phase when its fraction is small.

3) The microstructure of the composites with low volume fractions of TiNi matrix showed the presence of pores or even cracks formed in specimens of WC-43vol%TiNi, WC-20vol%TiNi and TiC-20vol%TiNi, which negatively affected the wear resistance of the composites. No pores formed in WC-Co regardless of the volume fraction of Co matrix, leading to higher wear resistance than composites with low volumetric TiNi matrix.

References

[1] T. Li, Q. Li, J.Y.H. Fuh, P.C. Yu and C.C. Wu, Effects of lower cobalt binder concentrations in sintering of tungsten carbide, Materials Science and Engineering A, 430 (2006) 113-119

[2] H. Saito, A. Iwabuchi, T. Shimizu, Effects of Co content and WC grain size on wear of WC cemented carbide, Wear, 261 (2006) 126-132

[3] A. Ball, On the importance of work-hardening in the design of wear-resistant materials, Wear, 91 (1983) 201

[4] J, Jin and H, Wang, Wear resistance of Ni–Ti alloy, Acta Metall. Sin. A 1 (1988) 76

[5] Y. Shida and Y. Sugimoto, Water jet erosion behaviour of Ti–Ni binary alloys Wear 146 (1991) 219

[6] R.H. Richman, A.S. Rao and D.E. Hodgson, Cavitation erosion of two TiNi alloys Wear 157 (1992) 401

[7] P. Clayton, Tribological behaviour of a titanium–nickel alloy Wear 162–164 (1993) 202-210

[8] R.H. Richman, A.S. Rao and D. Kung, Cavitation erosion of NiTi explosively welded to steel Wear 181–183 (1995) 80

[9] J. Singh and T.T. Alpas, Dry sliding wear mechanisms in a $Ti_{50}Ni_{47}Fe_3$ intermetallic alloy, Wear 181–183 (1995) 302

[10] D.Y. Li, Wear behaviour of TiNi shape memory alloys, Scr. Mater. 34 (1996) 195

[11] Y.N. Liang, S.Z. Li, Y.B. Jin, W. Jin and S. Li, Wear behaviour of a TiNi alloy, Wear 198 (1996) 236

[12] H.C. Lin, H.M. Liao, J.L. He, K.M. Lin and K.C. Chen, Wear characteristics of TiNi shape memory alloys, Metall. Mater. Trans. A, 28A (1997) 1871

[13] Y. Suzuki and T. Kuroyanagi, Development and application of intermetallic compound, Titanium Zirconium 27 (1979) 67-73

[14] C.A. Zimmerly, T. Inal and R.H. Richman, Explosive welding of a near-equiatomic nickel–titanium alloy to low-carbon steel, Mater. Sci. Eng. A, 188 (1994) 251

[15] D.Y. Li, A new type of wear-resistant material: pseudo-elastic TiNi alloy, Wear 221 (1998) 116

[16] Q. Chen and D.Y. Li, A computational study of the improvement in wear resistance of a pseudoelastic TiNi matrix composite achieved by adding TiN nanoparticles, Smart Mater. Struct. 16 (2007) S63–S70

[17] Rong Liu, D.Y. Li, A finite element model study on wear resistance of pseudoelastic TiNi alloy, Materials Science and Engineering A, 277 (2000) 169–175

[18] H.Z. Ye, R. Liu, D.Y. Li and R. Eadie, Development of a New Wear-resistant Material: TiC/TiNi Composite, Scripta Materialia, 41-10 (1999) 1039-1045

[19] D.Y Li, Y.C. Luo, Effects of TiN nano-particles on porosity and wear behavior of TiC-TiNi tribo composite, Journal of Materials Science Letters, 20 (2001) 2249-2252

[20] H.Z. Ye, R. Liu, D.Y. Li and R. Eadie, Improvement in wear resistance of TiNi-based composites by hot isostatic pressing, Materials Science and Engineering A, 329-331 (2002) 750-755

[21] H.Z. Ye, R. Liu, D.Y. Li and R. Eadie, Influences of porosity on mechanical and wear performance of pseudoelastic TiNi-matrix composites, Chemistry and Materials Science, 10-2 (2001) 178-185

[22] H. Tanaka, Y. Kishida, and J. Moriyama, Standard Free Energies for the Formation of Uranium Iron Carbide ($UFeC_2$) and Uranium Tungsten Carbide (UWC_2) by Electromotive Force Measurements, Japan Inst. Metal, 37 (1973) 564-567

[23] X. H. Wang, M. Zhang, Z. D. Zou and S. Y. Qu, Microstructure and wear properties of TiC–VC reinforced iron based hardfacing layers, Materials Science and Technology, 22 (2006) 193-198

[24] Gopal S. Upadhyaya, Cemented Tungsten Carbides - Production, Properties, and Testing, William Andrew Publishing/Noyes, 1998

[25] H. Tanaka, Y. Kishida, and J. Moriyama, Plastic deformation behaviour in Ni_3Ti single crystals with $D0_{24}$ structure, 51 (2003) 2623-2637

Chapter 5

Summary and Possible future studies

Chapter 5 - Summary and possible future studies

5.1 Summary of the thesis studies

1) A near equi-atomic pseudo-elastic TiNi alloy was introduced as a second phase to the Co-matrix of WC-Co composite, a well-known type of tribo-composite, in order to improve the wear resistance of the matrix while keeping its functions for binding the reinforcing phase and providing desired toughness. It was demonstrated that the pseudo-elastic TiNi phase was present in the matrix although some decomposition occurred during sintering. The added pseudo-elastic TiNi phase helped to reinforce the Co matrix and could also render it tougher. A small amount of TiNi considerably improved the wear resistance of WC-Co composite (reached optimal performance around 10wt%TiNi).

2) When the added TiNi alloy exceeded the amount of 10 wt%, the positive effect of TiNi alloy was weakened due to the formation of pores, which could be responsible for the deterioration of wear resistance.

3) The pseudo-elastic TiNi alloy was directly used as the matrix to make WC-TiNi and TiC-TiNi composites. It was demonstrated that the wear resistance of WC-Co composite was inferior to those of WC-TiNi and TiC-TiNi composites when the volume fraction of the metal matrix was high, e.g., 60vol%.

4) The wear resistance of WC-Co composites increased when the volume fraction of Co was reduced; whereas the wear resistance of WC-TiNi and TiC-TiNi

composites decreased when the fractions of TiNi were reduced. WC-Co performed better than WC-TiNi and TiC-TiNi when the volume fraction of TiNi matrix was low. This could be ascribed to the fact that TiNi alloy may not be well retained as the matrix phase due to its lower compatibility and the formation of pores appears to be a main problem.

5) The microstructure of the composites with low volume fractions of TiNi matrix showed the presence of pores or even cracks formed in specimens of WC-43vol%TiNi, WC-20vol%TiNi and TiC-20vol%TiNi, which negatively affected the wear resistance of the composites. No pores formed in WC-Co regardless of the volume fraction of Co matrix, leading to higher wear resistance than composites with TiNi matrix.

5.2 Discussion about future work

The beneficial effect of the pseudoelastic TiNi alloy can be anticipated. However, the formation of pores has turned to be a major problem in sintering when the amount of TiNi added to the Co matrix of WC-Co is higher than 10wt% or when the volume fraction of TiNi matrix of WC-TiNi was low. Pores also formed in TiC-TiNi with low volume fractions of TiNi matrix

It is of importance to study the mechanism responsible for the formation of pores in these cases and identify governing factors in order to prevent the process. The following studies could be helpful:

1) Investigate the interface between carbides and metal matrix in detail, determine reactions among WC, Co and TiNi and formed compounds, which could be complicated because of the involvement of four elements.

2) The canning technique could help to mitigate the problem of pore formation during sintering. Since there are cavities in the green pellets after compacting, the gas in the HIP chamber may get into samples especially when high pressure is applied. Although the canning technique could not prevent pores from forming in chemical reactions, it could reduce the pores mainly in a physical way and lead to sintering with better densification.

3) Sintering condition is another subject to investigate, since the microstructures and corresponding properties of samples can vary with different sintering temperature and sintering pressure. In this thesis study, 1500^{o}C and 4000 psi are used in the HIP sintering process. However, this sintering condition may not be suitable for all samples. Optimization of the sintering condition could improve the performance of the sintered composites.

4) In reality, the wear situation is more complicated than the experimental condition and the types of wear can be hybrid other than solely sliding wear. Therefore, more tests would be conducted tailored to the capability of the laboratory. Different acidic or alkaline environment can be introduced into the sliding wear test; other types of tests, say slurry erosion test or sand blasting test can also be performed on the WC-Co-TiNi composites in order to provide a more comprehensive evaluation of their wear resistance.